# THERMAL AND PHOTOINITIATED ELECTRON TRANSFER IN COPPER(I) CONTAINING BINUCLEAR IONS

Kenneth Alfred Norton, Jr.
B.S., Rider College, 1974
M.S., Southern Illinois University, 1976

A dissertation submitted to the faculty
of the Oregon Graduate Center
in partial fulfillment of the
requirements for the degree
Doctor of Philosophy
in
Inorganic Chemistry

November, 1980

The dissertation "Thermal and Photoinitiated Electron Transfer in Copper(I) Containing Binuclear Ions" by Kenneth A. Norton has been examined and approved by the following Examination Committee:

James K. Hurst
Professor
Thesis Advisor

Thomas M. Loehr
Professor
Examination Committee Chairman

James J. Huntzicker
Associate Professor

Thomas G. Dunne
Associate Professor, Reed College

# DEDICATION

To everyone just trying to make a little sense of it all.

# ACKNOWLEDGMENTS

I wish to express my greatest thanks to Dr. James K. Hurst for his guidance, encouragement and patience during the course of this work and I express thanks to Joel Johnson for his help with the laser apparatus and to Nancy Golobish for typing this dissertation.

Thanks also to Brenda Henry and Lester Lee for their encouragement. I express appreciation to Dr. Thomas M. Loehr for his careful reading of this dissertation and the helpful comments and suggestions which he offered. Lastly, I wish to recognize the students, staff and faculty of the Oregon Graduate Center for making my stay hère a truly memorable one.

# TABLE OF CONTENTS

Page

Chapter

## LIST OF TABLES

# LIST OF FIGURES

## ABSTRACT

### Thermal and Photoinitiated Electron Transfer in Copper(I) Containing Binuclear Ions

Kenneth A. Norton, Ph.D.
Oregon Graduate Center, 1980

Supervising Professor: James K. Hurst

Copper(I) forms $\pi$ complexes with olefin-containing metal complexes in aqueous solution. Reduction of a series of pyridinepentaammineruthenium(III) ions, where L is a pyridine or 4-substituted pyridines, was studied. For the $(NH_3)_5Ru(III)$-4-vinylpyridine ion it is possible to measure separately preequilibrium binuclear ion formation and electron transfer. The electron transfer pathway is determined to be intramolecular from comparison with rate behavior of $(NH_3)_5Ru(III)$-4-ethylpyridine, Cu(I) and $(NH_3)_5Ru(III)$-pyridine, Cu(I) redox pairs. Rate parameters are also determined for the reverse reaction, Cu(II) catalyzed autoxidation of the $(NH_3)_5Ru(II)$-4-vinylpyridine ion. The redox equilibrium constant determined from the kinetic data agrees reasonably with that calculated from the redox potentials of the reactants. Qualitative models have been advanced from which it is suggested that the entropy of activation gives a measure of the probability for electron transfer in the activated complex, values near zero indicating that electron-tunneling is not rate-limiting. Cu(I)-olefin containing binuclear ions of

$(NH_3)_5Co(III)L$, where L is an alkylpyridine or alkylamine, undergo efficient intramolecular electron transfer when irradiated in the Cu(I)-olefin($\pi^*$) absorption band. The results of photoredox studies of a series of alkylamine and alkylpyridine containing binuclear ions are reported. The quantum yields for Co(II) production is shown to fall off monotonically for increasing number of methylene carbons in the chain. Binuclear ions containing polyisoprenyl bridging ligands were also investigated. Mixed solvent studies show decreased quantum yield with increasing ethanol content of the aqueous media. Medium and chain configuration effects are discussed.

# LIST OF ABBREVIATIONS

| Symbol | Designate |
|---|---|
| $A = NH_3$ | ammonia |
| Cu(II) | $[Cr(H_2O)_6]^{2+}$ ion |
| Cu(I) | $[Cu(H_2O)_6]^{+}$ ion |
| Cu(II) | $[Cu(H_2O)_6]^{2+}$ ion |
| vp | 4-vinylpyridine |
| etpy | 4-ethylpyridine |
| DMSO | dimethylsulfoxide |
| DMF | dimethylformamide |
| HTFA | trifluoroacetic acid |
| TFA | trifluoroacetate |
| TMS | tetramethylsilane |
| $\delta$ | chemical shift in ppm |
| $k_o$ | observed rate constant |
| c | molar extinction coefficient |
| $\Delta H^{\ddagger}_{o}$ | observed enthalpy of reaction |
| $\Delta H^{\ddagger}_{et}$ | enthalpy for intrinsic electron transfer |
| $\Delta S^{\ddagger}_{o}$ | entropy for intrinsic electron transfer |
| $\Delta S_{pc}$ | entropy for precursor stability |
| $\Delta H_{pc}$ | enthalpy for precursor stability |
| $A_5Ru(III)vp$ | 4-vinylpyridine pentaammineruthenium(III) ion |

| Symbol | Designate |
|---|---|
| $k_{2nd}$ | second order rate constant |
| Cr(III) | $[Cr(H_2O)_6]^{3+}$ ion |
| [ ] | concentration |
| $[\ \ ]_o$ | concentration at time o |
| Co(II) | $[Co(H_2O)_6]^{2+}$ ion |
| py | pyridine |
| L | any uncharged ligand |

# CHAPTER 1

# INTRODUCTION

Light-induced electron transfer processes are of primary importance in naturally occurring photosynthetic systems; understanding the mechanism(s) by which this process occurs is a major area of investigation as alternative means for energy conversion are sought.[1] Electron transfer between molecules is the most fundamental process in nature. Electron transfer between simple inorganic molecules, complex metalloenzymes involved in respiration, in addition to protein matrixed metalloporphyrins found in photosynthetic reaction centers, are a few of the important examples of this process.[1] Of the diverse areas where electron transfer events occur, none are more amenable for study than those between coordination complexes. The parameters that govern electron transfer processes, distance, kinetic and optical properties can be elucidated using simple model reactions in an attempt to understand more complex ones.

Interest in oxidation-reduction (redox) reactions of coordination compounds begain in the late 1940's and early 1950's when attention was focused on relatively simple electron transfer reactions where only an electron is exchanged between two metal centers. This attention was stimulated by the chemists' adoption of crystal field theory, which explained the color, magnetism and reactivity of metal ions.

In 1953, Taube, Myers and Rich observed that two general types of redox reactions could be identified.[4] If electron transfer occurs between an oxidant and reductant which, during the time required for redox, contains metal centers inert to substitution (i.e., no expansion of the primary coordination shell) such as

$$5H^+ + [Co(NH_3)_5Cl]^{2+} + [Ru(NH_3)_6]^{2+} \rightarrow 5NH_4^+ + [Co(H_2O)_6]^{2+} + [Ru(NH_3)_6]^{3+}$$

the reaction is termed an outer-sphere (o.s.) electron transfer reaction (see Figure 1).

Alternatively, if the redox partners are chosen properly and the reductant is capable of substitution in its primary coordination sphere, a bond may be formed between the redox partners giving rise to a binuclear ion intermediate (two metals sharing a common ligand). This reaction is thought to occur by either of two pathways.

$$[Cr(H_2O)_6]^{2+} + [Co(NH_3)_5Cl]^{2+} \rightarrow$$

$$[(NH_3)_5\text{-}Co\text{-}Cl\text{-}Cr(H_2O)_5]^{5+} \rightarrow [Co(H_2O_6]^{2+} + [Cr(H_2O)_5Cl]^{2+} + 5NH_4^+$$

One involves sequential electron transfer from $Cr^{2+}$ through a chloride bridge to the Co(III) center with subsequent breakage of the product Co(II)-chlorine bond. The other pathway comprises simple atom transfer of chlorine in a single reaction step. In either case the chlorine is retained in the primary coordination sphere of the Cr(III) product. These types of reactions are termed inner sphere (i.s.) electron transfer reactions. The two mechanisms (i.s. and o.s.) are illustrated in Figure 1.

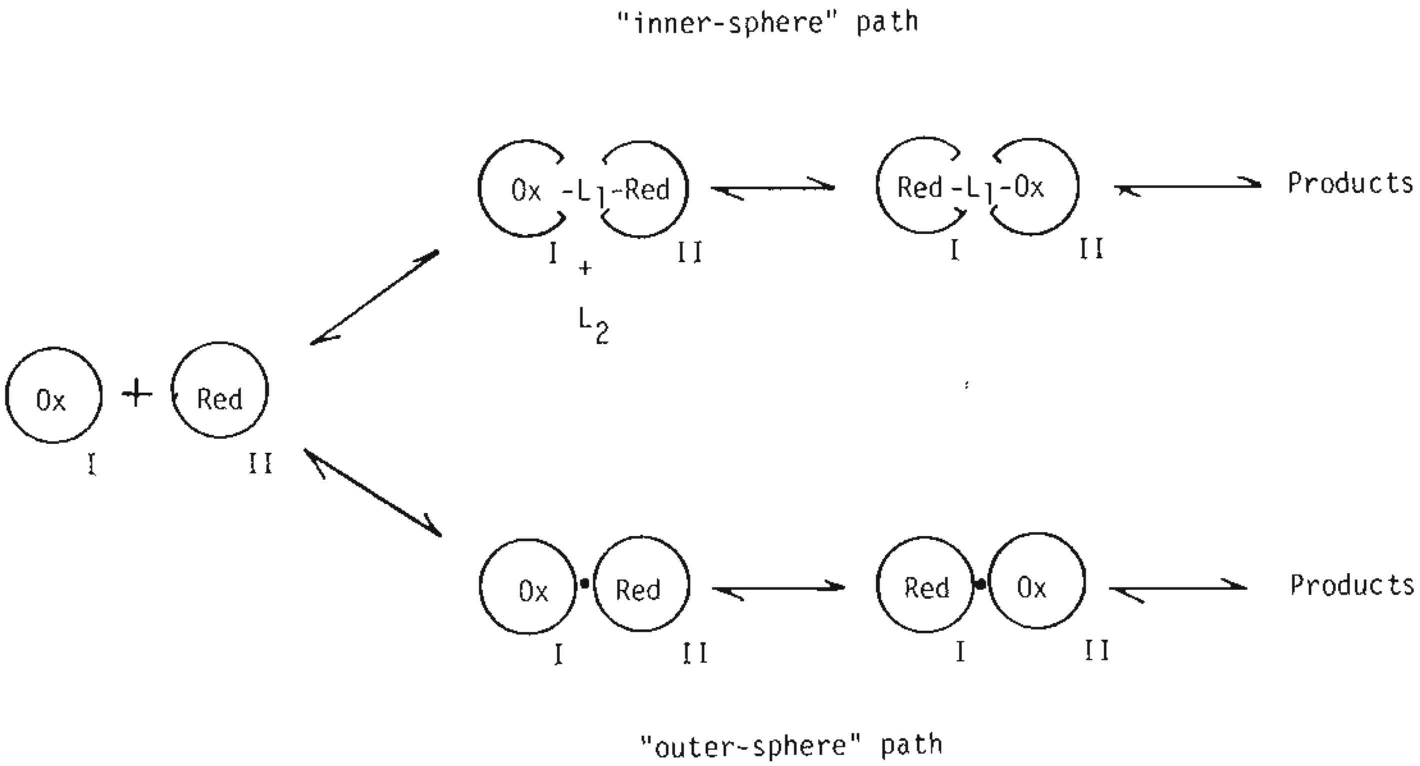

Figure 1. Schematic diagram of inner and outer sphere electron transfer pathways.

For inner sphere reactions there are three kinetic steps based upon Scheme I which may be rate limiting, giving rate restrictions summarized in Table 1.[3]

Scheme I.

$$Ox_I + Red_{II} \underset{k_{-1}}{\overset{k_1}{\rightleftharpoons}} (Ox_I\text{-}L_1\text{-}Red_{II})$$

$$[Ox_I\text{-}L_1\text{-}Red_{II}]^{\ddagger} \underset{k_{-2}}{\overset{k_2}{\rightleftharpoons}} [Red_I\text{-}L_1\text{-}Ox_{II}]$$

$$[Red_I\text{-}L_1\text{-}Ox_{II}] \underset{k_{-3}}{\overset{k_3}{\rightleftharpoons}} Red_I + Ox_{II}$$

TABLE 1

Kinetic Conditions for Rate Limiting Steps in

Electron Transfer Reactions

| Step | Conditions | Example |
|---|---|---|
| Precursor formation | $k_{-2} < k_1$ | $Fe^{2+}$ + *trans*$[Co(en)_2(H_2O)Cl]^{2+}$ |
| | $k_{-3} < k_2$ | |
| Electron transfer | $k_1 < k_{-2}$ | $V^{2+}$ + $[Co(NH_3)_5C_2O_4]^{+}$ |
| | $k_1 < k_{-2}k_{-3}/k_2$ | |
| Postcursor destruction | $k_3 < k_{-2}$ | $Cr^{2+}$ + $Ru(NH_3)_5Cl]^{2}$ |
| | $k_{-3} < k_2k_1/k_{-2}$ | |

An important requirement for understanding the rates of electron transfer is knowledge of the rates at which metal ions undergo substitution. This is important because in inner-sphere reactions it is the first step in the kinetic path. For octahedral metal-ion complexes substitution occurs via a dissociative process. This may be described as a reaction in which the rate limiting step involves dissociation of the ligand from the metal ion prior to bond-formation by the incoming ligand or complex.[4] The energy required for this process is mainly in the breakage of the metal-ligand in the transition state. Typically enthalpies of *ca*. 20-30 kcal/mole are required for these reactions at Co(III) and Ru(III) metal centers.

The rate at which ligand exchange occurs varies as a function of the electron configuration of the metal ions. For instance, the rates of $H_2O$ exchange in the primary coordination spheres of $Cr^{2+}$ and $Cr^{3+}$ differ by fifteen orders of magnitude. The exchange rates for water in $V^{2+}$ and $V^{3+}$ differ by a factor of 10.[2] This demonstrates that for inner sphere reactions, choice of redox partners is an important factor in precursor complex formation.

For most electron transfer reactions studied, the rate-determining step is the actual transfer of an electron and the intermediate does not accumulate. Equation 1 defines the measured rate constant, $k_o$, for just such a reaction, where $K_{pc}$ is the stability constant for precursor complex formation and $k_{et}$ the rate constant for electron transfer.

$$k_{obs} = k_{pc} \cdot K_{et} \qquad (1)$$

Measured rate parameters therefore give composite enthalpies and entropies (equations 2a, 2b).

$$\Delta H^{\ddagger}_{o} = \Delta H_{pc} + \Delta H^{\ddagger}_{et} \tag{2a}$$

$$\Delta S^{\ddagger}_{o} = \Delta S_{pc} + \Delta S^{\ddagger}_{et} \tag{2b}$$

Typical activation parameters for electron transfer reactions are listed in Table 2. Usually for ions of like charge $\Delta S^{\ddagger}_{o}$ is quite negative and $\Delta H^{\ddagger}_{o}$ is a small positive number. As mentioned previously, transition metal ion substitution enthalpies are much higher. Taube suggested that anomalously low enthalpy values ($\Delta H^{\ddagger}_{o}$) of electron transfer reactions could be rationalized by large negative values for $\Delta H_{pc}$.[5] The choice of a metal center which allows rapid equilibrium prior to electron transfer allowing the intermediate to accumulate is therefore necessary to study the intrinsic electron transfer step.

Precursor stabilities have not been amenable to study in many systems to date. Those systems which have been studied are presented in Table 3.[6-11] It is evident that precursor complex stability constants can span 10 orders of magnitude. From equation 1 it is seen that $K_{pc}$ is a contributor to the observed activation parameters. It is therefore necessary to separate this precursor formation term from the rate for electron transfer to determine the parameters for a given step. From Table 3 it can be seen that activation parameters for both inner and outer sphere processes can overlap and little can be said about the thermodynamic parameters for intrinsic electron transfer.

## TABLE 2

### Representative Activation Parameters for Electron Transfer[a]

| Reaction | ΔH‡ (Kcal/mole) | ΔS‡ (e.u.) |
|---|---|---|
| A. Outer-sphere | | |
| $Co(en)_3^{2+}$ - $Co(en)_3^{3+}$ | 13.7 | -33 |
| $Cr^{2+}$ - $Co(NH_3)_6^{3+}$ | 14.7 | -30 |
| $Cr(dipy)_3^{2+}$ - $Co(NH_3)_6^{3+}$ | 13.0 | -10 |
| B. Inner-sphere | | |
| $Cr^{2+}$ - $Cr(NH_3)_5F^{2+}$ | 13.4 | -30 |
| $Cr^{2+}$ - $Co(NH_3)_5OH_2^{3+}$ | 2.9 | -52 |
| $Cr^{2+}$ - $Co(NH_3)_5fumarate^{2+}$ | 7.5 | -33 |
| C. Uncertain mechanism | | |
| $Fe^{2+}$ - $Fe^{3+}$ | 9.4 | -25 |
| $Fe^{2+}$ - $Fe(phen)_3$ | 0.2 | -40 |
| $V^{2+}$ - $V^{3+}$ | 12.6 | -25 |

[a] Taken from reference 3.

## TABLE 3

### Magnitudes of Precursor Stability Constants

| Equilibrium | K($M^{-1}$) | Reference |
|---|---|---|
| $Ru(NH_3)_5OH_2^{2+} + CrCl^{2+} \rightleftharpoons [(NH_3)_5Ru(II)ClCr(III)]^{4+}$ | $4 \times 10^{-4}$ | 6 |
| $Ru^{2+} + CrCl^{2+} \rightleftharpoons [Ru(II)ClCr(III)]^{4+}$ | $1.4 \times 10^{-4}$ | 7 |
| $Cr^{2+} + Co(NH_3)_5OH^{2+} \rightleftharpoons [(NH_3)_5Co(III)\text{-}OH\text{-}Cr(II)]^{4+}$ | 0.1 - 10 | 8 |
| $(NH_3)_5RuOH_2^{2+} + (NH_3)_5RuN_2^{2+} \rightleftharpoons [(NH_3)_5RuN_2Ru(NH_3)_5]^{4+}$ | $7 \times 10^{3}$ | 9 |
| $(NH_3)_5CoO_2CCH{=}CH_2^{2+} + Cu^{+} \rightleftharpoons [(NH_3)_5Co(III)(O_2CCH{=}CH_2)Cu(I)]^{3+}$ | $4 \times 10^{4}$ | 10 |
| $(NH_3)_5$Co-nitrilotriacetate + $Fe^{2+} \rightleftharpoons [(NH_3)_5Co(III)NTAFe(II)]^{2+}$ | $1 \times 10^{6}$ | 11 |

We have taken advantage of the high affinity of Cu(I) for olefin bonds to determine separate precursor formation and electron transfer parameters.[10,12,13,16] Very large spectral changes occur upon coordination of Cu(I) to olefin bonds. These intense bands are due to Cu(I) → olefin ($\pi^*$) charge transfer.[10] Complexation corresponding to 1:1 binding stoichiometry is observed. Stability constants are on the order of magnitude $10^3$-$10^4$ and are dependent upon functional derivatives attached to the olefin.[10] The use of olefins attached to carboxylates, pyridines or amines which are coordinated to metal centers allows for formation of binuclear complexes in solution. In addition, Cu(II) does not complicate the system, for it forms no coordinated species with olefins.

It is also important to realize that there is an advantage in studying intramolecular as opposed to intermolecular electron transfer processes. Understanding the $\Delta H^{\ddagger}_{et}$ and $\Delta S^{\ddagger}_{et}$ of the reactions is the key to understanding the mechanism of the process; for example, values for assembling the ions cannot be separated out in intermolecular processes, and the influence of this assembly is particularly pronounced for highly charged ions.[1,13] To attempt to discuss effects attributable only to the electron transfer process, it is obviously easier to use systems where such precursor formation con-constants have been resolved. Having separated these terms, attention can be focused on the mechanism of electron transfer. In particular, the $\Delta S^{\ddagger}_{et}$ gives an indication of whether rate-limiting electron tunneling is important; negative values would support this mechanism, whereas strong overlap of orbitals would give rise to entropy values of near zero. Associated with thermal electron transfer processes is an optical promotion of the electron between centers corresponding to metal-to-metal charge transfer.[14,15] Investigation of systems where both thermal and optical redox properties can be observed will be important in resolving which theories best fit the available data.[14,15] Alkyl pyridinepentaammineruthenium(III) ions were chosen for studies of thermal and optical electron transfer parameters in redox reactions with Cu(I) in an attempt to determine the mechanism of electron transfer for the 4-vinylpyridinepentaaminerruthernium(III) ion.

Therefore, intramolecular processes can be used as a beginning to understand intermolecular processes where the distance between reacting centers has always been a parameter difficult to measure. Limits on this are very important in biological systems where intermolecular reactions are dominant and strong overlap of donor and acceptor orbitals is unlikely in redox pairs. It has been demonstrated that Cu(I)-Co(III) containing binuclear ions undergo photoinitiated electron transfer when irradiated in the metal to ligand charge transfer band (MLCT) of the Cu(I)-olefin-$\pi$-complexes.[16] By systematic structuring of the $(NH_3)_5Co(III)L$ ligand it is possible to construct binuclear ions where the median distance between the two reactive centers is varied in a regular manner. Ultimately this information (in addition to excited state information) can yield the distance limits for efficient photoredox processes in aqueous solution. In addition, π-conjugation has been proposed to mediate electron transfer; theoretical models have been advanced which are based on stacking or polyisoprenyl chains to form π-channels which facilitate electron transfer.[17] Binuclear Cu(I)-Co(III) ions containing polyisoprenyl ligands can be constructed. Results of studies in solutions of varying solvent composition which can perturb the ligand conformation should result in information helpful to determine whether or not specific polyisoprenyl chain configurations give rise to facile photoinitiated electron transfer. The results of investigations using Cu(I)-olefin π-coordinated binuclear ions are presented in this dissertation.

# CHAPTER 2

# EXPERIMENTAL

## Alkyl Bromides

When not commercially available, alkyl bromides were synthesized from the corresponding alcohols by the method of Wiley et al.[18] Usually 70 g (0.26 mol) of triphenylphosphine are dissolved in 250 ml of methylene chloride under nitrogen, cooled in an ice bath and 14 ml (0.26 mol) of bromine is added over 20 min with stirring. Pyridine (21.6 ml, 0.26 mol) is added and the alkyl alcohol (0.26 mol) is added dropwise over 30 min. The ice bath is removed and the solution allowed to warm for 90 min. The methylene chloride is removed by rotary evaporation and the resulting gelatinous mass extracted with pentane. The pentane solution is chilled in a dry ice-acetone bath and the residual triphenylphosphine oxide is filtered. The pentane is removed by rotary evaporation. Proton NMR was used to determine purity. Without exception, no proton shift was found corresponding to an alcohol. Proton (2H) NMR shifts corresponding to a terminal bromide (3.28-3.32 ppm) on methylene were found.

## 4-Alkylpyridine Ligands

Alkyl pyridines were synthesized by reacting the $C_{n-1}$ alkyl bromide with 4-methylpyridine using the method of Brown & Murphy.[19] In liquid ammonia, under nitrogen, a slight excess of 4-methylpyridine (12.9 ml, 0.132 mol) was added to $NaNH_2$ (5.2 g, 0.13 mol), the mixture was stirred for 30 minutes and the alkyl bromide (0.130 mol) added over a period of 90 min. The solution was stirred until the ammonia had evaporated. To the organic phase, 50 ml of water was carefully added and the solution extracted with ether. The ether phase was dried ($MgSO_4$), decolorizing carbon added and the solution filtered. The ether was removed by rotary evaporation and the crude 4-alkylpyridine was distilled under reduced pressure. In general it was not necessary to purify further the straight chain derivatives; with isoprene-containing derivatives, silica gel chromatography was necessary to insure a pure product. Chromatographic purification was made on silica gel 60, 70-230 mesh (E. Merck) using chloroform: ethyl acetate = 9:1 (v,v) as eluent. Yields were typically 65% of a colorless liquid although lower yields were obtained for the isoprene derivatives. Physical characterization of the individual ligands synthesized and preparatory notes are listed below.

4-(3-Butenyl)pyridine: b.p. 55°C (1.5 mm); $^1H$ NMR ($CDCl_3$) $\delta$ 8.40 (d, 2H, pyH), 1.04 (d, 2H, pyH), 5.7 (m, 1H, vinyl), 5.04 (s, 1H, vinyl), 4.9 (d, 1H, vinyl), 2.63 (t, 2H), 2.36 (t, 2H).

4-(4-Pentenyl)pyridine: b.p. 80°C (0.75 mm), $^1H$ NMR ($CDCl_3$) $\delta$ 8.41 (d, 2H, pyH), 7.05 (d, 2H, pyH), 5.70 (m, 1H, vinyl), 5.04 (s, 1H, vinyl), 4.90 (s, 1H, vinyl), 2.76 (m, 4H).

*4-(5-Hexenyl)pyridine*: b.p. 72°C (0.15 mm), $^1$H NMR ($CDCl_3$) δ 8.40 (d, 2H, pyH), 7.05 (d, 2H, pyH), 5.73 (m, 1H, vinyl), 5.00 (d, 1H, vinyl), 4.85 (s, 1H, vinyl), 2.58 (s, 2H), 2.06 (qrt. 2H), 1.50 (m, 2H).

*4-(6-Heptenyl)pyridine*: b.p. 92°C (0.40 mm), $^1$H NMR ($CDCl_3$), δ 8.38 (d, 2H, pyH), 7.07 (d, 2H, pyH), 5.69 (m, 1H, vinyl), 4.86 (d, 1H, vinyl), 4.81 (s, 1H, vinyl), 4.51 (d, 2H), 2.5 (s, 2H), 1.98 (d, 2H), 1.36 (s, 4H).

*4-(8-Nonenyl)pyridine*: b.p. 94°C (0.14 mm), $^1$H NMR ($CDCl_3$) δ 8.40 (d, 2H, pyH), 7.04 (d, 2H, pyH), 5.76 (m, 1H, vinyl), 4.99 (d, 1H, vinyl), 4.83 (s, 1H, vinyl), 2.56 (5, 2H), 1.98 (s, 2H), 1.58 (d, 2H), 1.38 (s, 8H).

*4-(10-Undecenyl)pyridine*: b.p. 120°C (0.15 mm); $^1$H NMR ($CDCl_3$) δ 8.39 (d, 2H, pyH), 7.00 (d, 2H, pyH), 5.76 (m, 1H, vinyl), 4.96 (d, 1H, vinyl), 4.81 (s, 1H, vinyl), 2.54 (s, 2H), 1.99 (d, 2H), 1.56 (s, 2H), 1.28 (s, 10H).

*4-(4', 8'-Dimethyl-3'(E), 7'-nonadienyl)pyridine (geranylpicoline)*: b.p. 134°C (0.75 mm). Column chromatography of silica gel was employed to remove a yellow impurity after distillation. $^1$H NMR ($CCl_4$) δ 8.41 (d, 2H, pyH), 7.04 (d, 2H, pyH), 5.11 (s, 2H, vinyl), 2.62 (s, 2H), 2.36 (t, 2H, 2.04 (s, 4H), 2.70 (s, 3H), 2.64 (s, 3H), 2.59 (d, 6H).

4-(4',3',12'-Trimethyl-3'(E), 7'(E), 11'-tridecatrienyl)pyridine (farnesylpicoline): b.p. 153°C (0.15 mm). Column chromatography on silica gel was necessary after distillation to remove a yellow impurity. $^1$H NMR (CCl$_4$) $\delta$ (d, 2H, pyH), 7.02 (d, 2H, pyH), 5.04 (s, 3H, vinyl), 2.6 (t, 2H), 2.32 (t, 2H), 2.0 (s, 8H), 2.64, 2.59, 2.51 (s's, 12H).

## Aminoalkenes

Aminoalkenes were prepared by the method of Roberts & Mazur.[20] The $C_n$ alkyl bromide (0.26 mol) was dissolved with stirring in 150 ml of DMF with a slight excess of potassium phthalimide (48.5 g, 0.27 mol), heated under nitrogen to 120°C for 30 min, then at 160°C for 30 min. The mixture was poured over 200 g of ice and extracted with three 50 ml volumes of chloroform. The chloroform layer was washed with 1 M potassium hydroxide, 0.5 M hydrochloric acid and twice with water. The chloroform layer was dried (Na$_2$SO$_4$) and the chloroform removed by rotary evaporation.

The resulting crude N-alkylphthalimide was dissolved in 95% ethanol and a slight excess of hydrazine hydrate added. The solution was refluxed for an hour, cooled in an ice bath, an excess of hydrochloric acid added and the solution filtered. The phthalhydrazide remaining in the filter was washed with three 100 ml fractions of water and the water removed *in vacuo*.

The resulting amine hydrochloride was dissolved in aqueous potassium hydroxide at pH 10 and extracted with three 25 ml portions of ether. The ether layer was dried ($MgSO_4$) and the ether removed by rotary evaporation. The crude amine was distilled over potassium hydroxide. Physical characterizations of the individual ligands are listed below.

*1-Amino-4-pentene*: ($NH_2(CH_2)_3CH{=}CH_2$), $^1$H NMR ($CDCl_3$) $\delta$ 5.69 (m, 1H, vinyl), 5.01 (d, 1H, vinyl), 4.83 (s, 1H, vinyl), 2.68 (t, 2H), 2.08 (qrt, 2H), 1.75 (s, 2H), 1.56 (qrt, 2H).

*1-Amino-5-hexene*: ($NH_2(CH_2)_4CH{=}CH_2$), b.p. 128 (760 mm), $^1$H NMR ($CDCl_3$) $\delta$ 5.74 (m, 1H, vinyl), 4.98 (d, 1H, vinyl), 4.84 (s, 1H, vinyl), 2.66 (5, 2H), 2.00 (d, 2H), 1.40 (t, 8H).

*1-Amino-7-octene*: ($NH_2(CH_2)_6CH{=}CH_2$), $^1$H NMR ($CDCl_3$), $\delta$ 5.76 (m, 1H, vinyl), 4.98 (d, 1H, vinyl), 4.84 (s, 1H, vinyl), 2.66 (d, 2H), 2.00 (d, 2H), 1.33 (s, 10H).

*1-Amino-9-decene*: ($NH_2(CH_2)_8CH{=}CH_2$), $^1$H NMR ($CDCl_3$), $\delta$ 5.76 (m, 1H, vinyl), 4.98 (d, 1H, vinyl), 4.82 (s, 1H, vinyl), 2.64 (d, 2H), 2.01 (d, 2H), 1.30 (s, 12H).

*1-Amino-3,7-dimethyl-2(E),6-octadiene (Geranylamine)*:

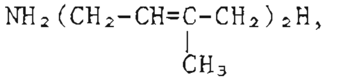

$NH_2(CH_2\text{-}CH{=}\underset{\displaystyle CH_3}{\underset{|}{C}}\text{-}CH_2)_2H$, b.p. 67°C (0.45 mm), $^1$H NMR ($CDCl_3$) $\delta$ 5.10 (d, 1H, vinyl), 4.61 (s, 1H, vinyl), 3.21 (d, 2H), 2.68 (s, 2H), 2.08 (s, 4H), 1.66, 1.59 (s, s, 12H), 1.12 (s, 2H, amine).

1-Amino-3,7,11-trimethyl-2(E),6(E),10-dodecatriene (farnesylamine): 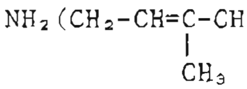
$NH_2(CH_2\text{-}CH{=}\underset{\displaystyle CH_3}{\underset{|}{C}}\text{-}CH_2)_3H$, b.p. 117°C (0.60 mm), $^1$H NMR ($CDCl_3$), δ 5.16 (d, 2H, vinyl), 4.66 (s, 1H, vinyl), 3.26 (d, 2H), 2.68 (s, 2H), 2.04 (s, 4H), 1.67, 1.60 (s, s, 16H), 1.16 (s, 2H, amine).

## Isomeric 5-methylbicyclo[2.2.2.]oct-2-ene-5-carboxylic acids (bicyclooctene carboxylic acids) ($C_{10}H_{14}O_2$)

The isomeric acids were prepared by the method of Boehme et al.[21] 1,3-Cyclohexadiene (49 g, 0.61 mol), methacrylic acid (55 g, 0.64 mol) and hydroquinone (1 g) were heated in a sealed tube at 160°C for 14 hours. The crude mixture was vacuum distilled and 27.91 g (31% yield) of a white solid was collected. The product was recrystallized from pentene.

## 5-*exo*-Methylbicyclo[2.2.2]oct-2-ene-5-*endo*-carboxylic acid

Iodolactone procedure: The isomers were separated by converting the *endo*-carboxylic acid to its corresponding iodolactone.[21] The isomeric mixture (26 g, 0.15 mol) was neutralized with NaOH and diluted to 1000 ml in aqueous 0.5 N sodium bicarbonate. To this solution was added 500 ml of aqueous potassium iodide (83 g, 0.5 mol) and molecular iodine (42.6 g, 0.17 mol). The solution was placed in the dark, stirred for 3 hours and allowed to stand overnight. The brown precipitate which had settled was filtered and washed with water, dissolved in chloroform, and washed with 10% aqueous sodium thiosulfate until two clear phases obtained. The chloroform was removed by rotary evaporation leaving a yellowish solid.

### 5-*endo*-Methylbicyclo[2.2.2.]oct-2-ene-5-*exo*-carboxylic acid

The aqueous bicarbonate solution from the iodolactone procedure was titrated with solid sodium thiosulfate and acidified with hydrochloric acid. The precipitated *exo*-carboxylic acid was filtered, washed with water, dissolved in pentane, dried ($MgSO_4$) and cooled to -20°C to induce precipitation. The product was dried in a vacuum desiccator over anhydrous $CaSO_4$. Yield: 6.4 g (50%).

The $^1H$ NMR spectrum ($CDCl_3$) gave the following: $\delta$ 6.24 (m, 2H, olefin), 2.75 (m, 1H), 2.54 (s, 1H), 2.40 (d, 1H), 1.64 (m, 1H), 1.55 (m, 1H), ~ 1.2 (m, 2H), 1.13 (s, 3H, Me), 0.98 (m, 1H).

### 5-*exo*-Methylbicyclo[2.2.2.]oct-2-ene-5-*endo*-carboxylic acid

The iodolactone and zinc dust (40 g) were refluxed overnight in 150 ml of ethanol. The solution was filtered and the ethanol removed by rotary evaporation. The crude *endo* product was dissolved in dilute sodium hydroxide, filtered, precipitated by addition of hydrochloric acid, filtered, dissolved in pentane, dried by adding anhydrous $MgSO_4$ and the pentane removed by rotary evaporation. Yield: 5.2 g (40%).

The $^1H$ NMR spectrum ($CDCl_3$) gave: $\delta$ 6.23 (m, 2H, olefin), 2.70 (m, 1H), 2.52 (m, 1H), 2.28 (m, 1H), 2.15 (m, 1H), 1.82 (m, 1H), 1.75 (m, 1H), 1.32 (s, 3H, Me), 1.21 (m, 1H), 1.08 (m, 1H).

## Ruthenium Coordination Complexes

*General Procedure*: Approximately 200 mg (0.68 mM) of $[Ru(NH_3)_5Cl]Cl_2$ in 15 ml of dilute HTFA (pH 4-5) (scheme II) was reduced under argon and transferred anaerobically to an argon-flushed solution containing the ligand in ethanol (1:3 v/v). The solution was cooled in an ice bath and extracted twice with ether. The complex was precipitated by adding solid ammonium hexafluorophosphate. The complex was then twice recrystallized from warm water (40-45°C) and washed with ethanol and ether. The ruthenium complex was oxidized by stoichiometric addition of silver oxide, dissolved in HTFA (The $Ag_2O$ was first added to 0.5 ml of HTFA and diluted to about 5 ml with $H_2O$.). The mixture was cooled in an ice bath and filtered through Celite to remove the solid AgO which formed. To the filtrate was added solid sodium perchlorate and the volume reduced under vacuum at 40-50°C until the complex precipitated. The product $[Ru(HN_3)_5L](ClO_4)_3$ was recrystallized from warm water and washed with ethanol, ether, and dried under vacuum over anhydrous $CaSO_4$. Yields were generally 80-125 mg (20-30% based on Ru content).[13] Spectral properties are summarized in Table 4.

*4-Vinylpyridinepentaammineruthenium(III) perchlorate $[Ru(NH_3)_5(4\text{-vinylpyridine})](ClO_4)_3$*: Synthesis of this complex was plagued with many problems until the explicit procedure described above was adopted. Polymerization of the ligand during complexation was

Scheme II.

$$\begin{tikzcd}
{[Ru(NH_3)_5Cl]Cl_2} \arrow[r, "Zn(Hg)"] & {[Ru(NH_3)_5Cl]^{+}} \arrow[r, "L"] & {[Ru(NH_3)_5L]^{2+}} \arrow[d, "PF_6^-"] \\
{[Ru(NH_3)_5L]^{3+} + Ag^{\circ}(s)} \arrow[d, "ClO_4^-"] & & {[Ru(NH_3)_5L](PF_6)_2} \arrow[ll, "AgTFA"'] \\
{[Ru(NH_3)_5L](ClO_4)_3} & &
\end{tikzcd}$$

TABLE 4

Spectral Properties of $[Ru(NH_3)_5L]^{2+,3+}$[a]

| L | $[Ru(NH_3)_5L](PF_6)_2$ | | $[Ru(NH_3)_5L](ClO_4)_3$ | |
|---|---|---|---|---|
| | $\lambda_{max}$ | $\varepsilon \times 10^{-3}$ | $\lambda_{max}$ | $\varepsilon \times 10^{-3}$ |
| 4-vinylpyridine | 453 | 9.9 | 420 | 0.47 |
| | 255 | 9.3 | 317 | 4.3 |
| | 241 | 12.2 | 251 | 12.0 |
| 4-ethylpyridine | 394 | 5.0 | 251 | 6.04 |
| | 245 | 6.5 | | |
| pyridine | 407 | 7.8 | 261 | 4.7 |
| | 245 | 4.6 | 255 | 4.7 |
| | | | 248 | 4.7 |

[a] All measurements at 24°C in 0.1 M TFA, wavelengths in nm.

minimized by using glassware which had been first soaked in sodium dichromate-sulfuric acid, rinsed with nitric acid and then with deionized water. Initial attempts at synthesis using silver ion to precipitate the chloride counter-ions of $(NH_3)_5RuCl_3$ were abandoned to reduce the possibility of Ag(I) ion interfering with complexation and subsequent reaction steps. Maintaining the acidity at pH 4-5 reduced the extent of formation of decomposition and polymerization products in the initial isolation step, helped increase shelf life and resulted in reliable kinetic behavior from preparation to preparation. Synthesized by the above method, the Ru(III) salt was stable at 0°C for several days as judged by kinetic behavior. The Ru(II) salt was stable for longer periods of time when stored at 0°C. Elemental analysis for the Ru(II) salt: Calcd: C, 14.46; H, 3.81; N, 14.46. Found: C, 14.40; H, 4.00; N, 14.49. The $^1H$ NMR spectrum of the Ru(II) salt in $(Ch_3)_2SO\text{-}d_6$ was nearly identical with that for uncomplexed 4-vinylpyridine, the pyridine resonance bands being broadened slightly and shifted downfield $\delta$ 0.03 ppm by coordination. Additional broad bands from *trans*- and *cis*-$NH_3$ protons appeared at $\delta$ 2.95 and 2.30 respectively. Electronic spectra are given in Table 4.

Pyridinepentaammineruthenium(III) perchlorate $[Ru(NH_3)_5(pyridine)](ClO_4)_3$: The general procedure described above was followed with the exception that ethanol addition was not necessary to insure solution homogeneity in the initial complexation step. $^1H$ NMR in

$(CH_3)_2SO$-$d_6$ showed results similar to the vinylpyridine complex, the pyridine protons being shifted downfield and slightly broadened by complexation. Electronic spectra are reported in Table 3. These values agree with previous reported values.

4-Ethylpyridinepentaamineruthenium(III) $[Ru(NH_3)_5$ (4-ethylpyridine)] $(ClO_4)_3$: The general procedure described above was followed. Again $^1H$ NMR in $(CH_3)_2SO$-$d_6$ showed pyridine ring protons shifted downfield and broadened. Electronic spectra are reported in Table 3.

## Cobalt 4-Alkylpyridine Coordination Complexes

General Procedure: Complexes of different alkylpyridine derivatives were prepared by heating dimethylsulfoxidepentaamminecobalt(III) perchlorate ($(NH_3)_5Co(III)DMSO$, 2 g) with the ligand in 10 ml of dimethylsulfoxide (DMSO) or dimethylformamide (DMF) at 60°C for four hours. Molecular sieve was added to exclude moisture and the solution stirred continuously under nitrogen to prevent oxidation of the ligand. To the product solution was added 10 ml of $H_2O$, the molecular sieve filtered off, the aqueous phase extracted three times with ether, and 0.1 M $HClO_4$ and solid $NaClO_4$ were added to induce complex precipitation. The solution was filtered and the complex recrystallized from warm water until the electronic spectrum showed no trace of $[Co(NH_3)_5(DMSO)]^{3+}$, $[Co(NH_3)_5(DMF)]^{3+}$, $[Co(NH_3)_5(OH_2)^{3+}]$ ions. The $^1H$ NMR spectra were similar to those of the uncomplexed ligands with the exception of shifting of the pyridine protons found at 8.20 and

TABLE 5

Visible Electronic Spectra of $[Co(NH_3)_5L](ClO_4)_3$

Complexes of Alkyl Pyridines[a]

| L | $\lambda(\varepsilon_\lambda)$ | |
|---|---|---|
| 4-(3-Butenyl)pyridine | 340(69) | 473(70) |
| 4-(4-Pentenyl)pyridine | 340(71) | 472(64) |
| 4-(5-Hexenyl)pyridine | 340(68) | 473(73) |
| 4-(6-Heptenyl)pyridine | 340(71) | 473(69) |
| 4-(8-Nonenyl)pyridine | | 473(67) |
| 4-(10-Undecenyl)pyridine | | 474(70) |
| Geranylpicoline | | 472(71)[b] |
| Farnesylpicoline | | 470(73)[b] |

[a] Absorbances in 0.1 M HTFA unless noted otherwise.

[b] 0.1 M $HClO_4$ in 75% ethanol.

7.04 to 8.25 and 7.65 ppm, respectively, and the appearance of protons assignable to *cis*- and *trans*-coordinated amines at 3.21 and 3.68 ppm. All complexes exhibited electronic spectra consistent with coordinated pyridine; spectral data for alkylpyridine coordination complexes in 0.1 M trifluoroacetic acid are listed in Table 5. Preparatory notes for complexes are listed below.

4-Vinylpyridinepentaaminecobalt(III)perchlorate $[Co(NH_3)_5$-$(4\text{-Vinyl-pyridine}](ClO_4)_3$: This complex was prepared by equilibrating $[Co(NH_3)_5(DMSO)](ClO_2)_3$ (2g), DMF (6 ml) and molecular sieve at 60°C for 2 hours. 4-Vinylpyridine (2 ml) was added and the solution maintained at 60°C for 2 hours. The resulting solution was filtered, 10 ml of $H_2O$ added, extracted three times with ether, diluted with 10 ml of 0.1 M $HClO_4$ and solid sodium iodide added to induce complex precipitation. The iodide salt was recrystallized twice from warm water and converted to the perchlorate salt by stoichiometric addition of silver perchlorate ($AgClO_4$) and precipitated with 0.1 M $HClO_4$ and solid sodium perchlorate. The complex was recrystallized three times from dilute perchloric acid. Yield 573 mg (27%). The $^1H$ NMR spectrum gave results consistent with coordinated 4-vinyl pyridine, the pyridine protons being shifted to 8.38 and 7.78 ppm. In addition, *cis*- and *trans*-ammine protons appear at $\delta$ 3.65 and 3.45. The visible absorption spectrum was $\lambda(\varepsilon_\lambda)$ = 477(68), 344(77), in 0.1 M $HClO_4$.

$[Co(NH_3)_5(4\text{-}(3\text{-Butenyl})pyridine)](ClO_4)_3$: The general method described above was used. Electronic spectrum: $\lambda(\varepsilon_\lambda)$ = 340(69), 473 (70).

$[Co(NH_3)_5(4\text{-}(4\text{-Pentenyl})pyridine)](ClO_4)_3$: The general procedure described above was used. Electronic spectrum: $\lambda(\varepsilon_\lambda)$ = 340(71), 472 (64).

$[Co(NH_3)_5(4\text{-}(5\text{-Hexenyl})pyridine)](ClO_4)_3$: The general procedure described above was used. Electronic spectrum: $\lambda(\varepsilon_\lambda)$ = 340(68), 473 (73).

$[Co(NH_3)_5(4\text{-}(6\text{-Heptenyl})pyridine)](ClO_4)_3$: The general procedure described above was used with the following modification: For the final series of recrystallizations warm ethanol:water, 1:4 (v,v) was used. Electronic spectrum: $\lambda(\varepsilon_\lambda)$ = 340(81), 473(69).

$[Co(NH_3)_5(4\text{-}(8\text{-Nonenyl})pyridine)](ClO_4)_3$: The general procedure described above was used with the following exception: For the final series of recrystallizations a 50% warm ethanolic solution was used. Electronic spectrum: $\lambda(\varepsilon_\lambda)$ = 473(69).

$[Co(NH_3)_5(4\text{-}(10\text{-Undecenyl})pyridine)](ClO_4)_3$: The general procedure described above was used with the following modification. For the final series of recrystallizations warm 50% ethanol:water was used. Electronic spectrum: $\lambda(\varepsilon_\lambda)$ = 474(70).

[$Co(NH_3)_5$(Geranylpicoline)]$(ClO_4)_3$: The general procedure described above was used with the exception of 50% ethanol being used in the final recrystallization steps. It was also necessary to induce complex precipitation by reducing the volume of the solution containing the complex by rotary evaporation. Electronic spectrum: $\lambda(\varepsilon_\lambda)$ = 472(71) in 75% ethanol, 0.1 M $HClO_4$.

[$Co(NH_3)_5$(Farnesylpicoline)]$(ClO_4)_3$: The general procedure described above was used, with the modification listed for the [$Co(NH_3)_5$(Farnesylpicoline)]$(ClO_4)_3$. Electronic spectrum: $\lambda(\varepsilon_\lambda)$ = 470(73) in 75% ethanol 0.1 M $HClO_4$.

## Cobalt-Aminoalkene Coordination Complexes

General Procedure: Dimethylsulfoxidepentaamminecobalt(III) perchlorate (2 g) was stirred in 5 ml of dry DMSO or DMF under nitrogen in the presence of 2-3 ml of the alkylamine at 60°C for 2-3 hours. Molecular sieve was present to insure anhydrous conditions. The solution was filtered, diluted to 20 ml with $H_2O$, extracted twice with ether, and 10 ml of 0.1 M $HClO_4$ added with excess solid $NaClO_4$ to induce complex precipitation. The slurry was chilled (5-7°C), filtered, and the alkylaminecobalt perchlorate complex recrystallized twice from warm (50-60°C) water and washed with ethanol and ether. In the cases of longer chain alkylamines ($C_n$ = 8-15) it was necessary to recrystallize the complexes from 50% ethanol. Complexes were dried under vacuum over $CaSO_4$. The $^1H$ NMR spectra for spin-spin splitting of vinyl protons were nearly identical for $A_5Co$-complexes and the corresponding uncoordinated amines. The α-methylene protons of each ligand could be detected under the *cis*- and *trans*-ammines of the coordination complexes in $(CH_3)_2SO\text{-}d_6$. The amine peak of the free ligand disappeared in the metal ion complex. Alkyl-ligand methylenes other than the α-methylene peaks were not affected by complexation. The complexes were also characterized by visible absorption spectra which are listed in Table 6 and below under individual complex preparatory notes. (The spectra are recorded in 0.1 M $HClO_4$ unless noted otherwise.)

<u>$[Co(NH_3)_5(\text{1-Amino-4-pentene})](ClO_4)_3$</u>: The general procedure described above was used. Electronic spectrum: $\lambda(\varepsilon_\lambda) = 340(64)$, $477(63)$.

<u>$[Co(NH_3)_5(\text{1-Amino-5-hexene})](ClO_4)_3$</u>: The general procedure described above was used. This complex easily formed microcrystalline salts from warm water. Electronic spectrum: $\lambda(\varepsilon_\lambda) = 340(64)$, $477(65)$.

<u>$[Co(NH_3)_5(\text{1-Amino-7-octene})](ClO_4)_3$</u>: The general procedure described above was used. As mentioned above, it was necessary to recrystallize this complex from a 50% ethanol solution. Electronic spectrum: $\lambda(\varepsilon_\lambda) = 340(64)$, $477(66)$.

<u>$[Co(NH_3)_5(\text{1-Amino-9-decene})](ClO_4)_3$</u>: The general procedure described above was used. When the product solution was extracted

## TABLE 6

### Visible Electronic Spectra of $[Co(NH_3)_5L](ClO_4)_3$ Complexes of Alkylamines[a]

| L | $\lambda(\varepsilon_\lambda)$ | |
|---|---|---|
| 1-Amino-4-pentene | 340(64) | 477(63) |
| 1-Amino-5-hexene | 340(64) | 477(65) |
| 1-Amino-7-octene | 340(64) | 477(66) |
| 1-Amino-9-decene | 340(64) | 477(66) |
| Geranylamine | | 478(65)[b] |
| Farnesylamine | | 478(65)[b] |

[a] In 0.1 M $HClO_4$.

[b] In 0.1 M $HClO_4$, 75% aqueous ethanol.

with ether, it was found that back extraction of the complex from ether improved yields. This complex was recrystallized from 50% ethanol. Electronic spectrum: $\lambda(\varepsilon_\lambda)$ = 340(64), 477(66).

$[Co(NH_3)_5(\text{Geranylamine})](ClO_4)_3$: The general procedure described above was followed. This complex was somewhat flocculent in appearance when recrystallized from 50% ethanol. Electronic spectrum: $\lambda(\varepsilon_\lambda)$ = 478(65) in 75% ethanol.

$[Co(NH_3)_5(\text{Farnesylamine})](ClO_4)_3$: The general procedure described above was followed. Even after repeated recrystallization from 50% ethanol the complex did not give a well-defined state of appearance or texture, behaving similar to a wax. The electronic spectrum, $\lambda(\varepsilon_\lambda)$ = 478(65), and $^1H$ NMR were consistent with other alkylamine complexes, however.

### Other Reagents

Solvents employed were reagent grade or better and used as received. All ligands commercially available were distilled immediately before use. Aqueous solutions were prepared with reverse-osmosis deionized water. Stock solutions of cupric ion in trifluoroacetic acid (HTFA) were prepared by dissolving $Cu(ClO_4)_2$ in aqueous HTFA, then precipitating perchlorate by adding potassium hydroxide, leaving the solution 0.1 M in HTFA; Cu(II) concentrations were determined by the method of Kitson[23] which involves spectrophotometric determination of $Cu(SCN)_4$ ions. Solutions of $Cu(ClO_4)_2$ were prepared by mixing stoichiometric equivalents of cupric oxide and perchloric acid and adjusting the acidity to pH 1. Chromic trifluoroacetate reagent solutions were prepared by reducing primary standard dichromate in HTFA with hydrogen peroxide after addition of perchloric acid to precipitate potassium ion; Cr(III) concentrations were determined by oxidation to $CrO_4^{-2}$ with alkaline peroxide. Chromic perchlorate solutions were prepared by using $HClO_4$ in place of HTFA. Chromous ion solutions were obtained by anaerobic (argon) reduction with zinc-mercury amalgam. Cuprous ion was generated by reaction of Cr(II) with an excess of Cu(II) to insure complete oxidation of chromous ion.

# CHAPTER 3

# INSTRUMENTATION

## Kinetic Methods

Kinetic measurements with half-times of less than 15 seconds were made on a stopped-flow instrument of conventional design.[15] A lucite block, housing the optical tubes, was channeled to permit circulation of thermostatting coolant. Temperatures could be controlled to ± 0.1°C. The apparatus was fitted with reservoir chambers which allowed oxygen purging and direct loading of reactant solutions into the drive syringes in the mixing block without exposure to air. Transmittance changes were recorded on a Tektronix Model 549 recording oscilloscope, photographed and converted to absorbance for analysis.

Reactions with half-times greater than 15 seconds were recorded on a Cary 16 spectrophotometer. Reactions were initiated using anaerobic syringe transfer of the limiting reagent into serum-stoppered optical cells containing anaerobic solutions of the excess reagent. The cells containing the excess reagent were typically given at least 15 minutes to attain thermal equilibrium with the thermostatted cell compartment before reagent mixing. The rates were obtained by following light intensity changes in the visible absorption maxima for pentaammineruthenium(II) ions.

## Photochemical Methods

Illumination of samples was accomplished using a Hanovia 200 W high-pressure mercury-xenon compact arc lamp housed in a Bausch & Lomb mercury light source and powered by a Kepco regulated DC power supply. Light was passed through a Bausch & Lomb high intensity u.v. grating monochromator focused with an achromatic condenser lens, an ultraviolet cutoff filter to remove stray light, then through the reaction cell. Light intensities controlled with variable width slits, ranged over values $I_0 = 0.5 - 2.5 \times 10^{-9}$ einstein $sec^{-1}$ at 306 nm. An alternate source of illumination used for some of the measurements was a Q-switched Nd:YAG pulsed laser, which was frequency-doubled and dye-shifted (Kiton Red) to give excitation energy at 306 nm.[26] A schematic diagram is given in Figure 2. Light intensities were measured either with a bolometer[27] or by ferrioxalate actinometry.[28] The bolometer signal output was monitored over the course of the irradiation time and the intensity averaged. The intensity varied from $0.5 - 1.0 \times 10^{-8}$ einstein $sec^{-1}$. Cylindrical optical cells with 2 cm pathlength were used in the photolysis experiments.

## Other Methods

Ultraviolet and visible spectra were obtained on Cary 15 or Cary 16 (Varian) instruments and are reported in nm. Tandem difference cells were used for studies of the absorption spectrum of a binuclear reactant ion. Proton magnetic resonance spectra were obtained with

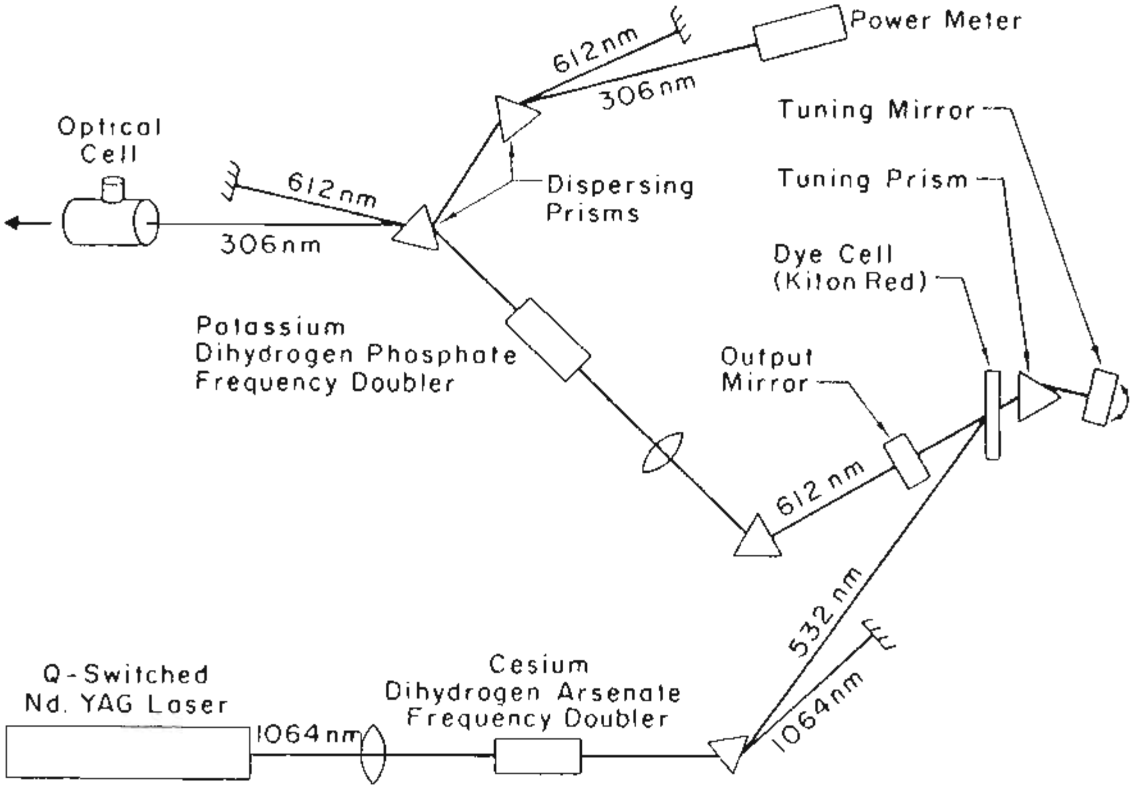

Figure 2. Near-ultraviolet laser energy source.

either a Varian Model H-100 or JEOL Model FX 90Q FT spectrometer using tetramethylsilane as an internal standard. Chemical shifts are reported in $\delta$ units. Elemental analyses were performed by Galbraith Laboratories, Knoxville, Tennessee. Gas chromatograms were produced using a Varian Model 1200 Series Aerograph in the isothermal mode equipped with either a Spectra Physics SP4100 computing integrator or a Linear chart recorder. The column material used for ligand analysis was 4% Carbowax 20 M, and 0.8% KOH on Carbopack B (Supelco, Inc.).

Cyclic voltammograms were measured on an instrument with a three electrode configuration: platinum wire, platinum foil and silver wire in 0.1 M silver nitrate were the working, counter and reference electrodes, respectively.

## Quantum Yield Calculations

The amount of Co(II) produced in photoredox reactions of Co(III)-Cu(I) binuclear ions was measured by the method of Kitson and by the disappearance of Co ← L charge transfer in the visible region. The amount of Co(II) as measured by each method agreed within experimental error. Blanks were run to determine the quantum yield for Co(II) produced by other processes (e.g., as formed from direct irradiation of u.v. Co ← L ($\pi^*$) charge transfer band). The Co(II) produced in these experiments was taken into account for correcting total Co(II) found for samples irradiated with Cu(I)-Co(III) binuclear ions. The quantum yield of Co(II) produced by Cu(I) → olefin irradiation was calculated with the following formula:

$$\Phi_{\mathrm{Cu(I)} \rightarrow \mathrm{olefin}} = [\mathrm{Co(II)}_T - \Phi_{op} \cdot (I_a)(1 - \bar{f})t]/I_a t\bar{f} \qquad (3)$$

where $I_a = I_o(1 - 10^{\epsilon cl})$ is the average number of photons per second absorbed; t is the irradiation time in seconds; $\bar{f}$ is the fraction of absorbed light which goes into the Cu(I) → olefin band; and $1 - \bar{f}$ is the light absorbed which goes into the Co(III) ← L($\pi$*) band. $\Phi_{op}$ is the quantum yield of Co(II) by direct irradiation of the Co(III) ← L($\pi$*) charge transfer band. $\Phi_{op}$ is calculated from

$$\Phi_{op} = [\mathrm{Co(II)}]/I_a tA \qquad (4)$$

where [Co(II)] is Co(II) found after an irradiation time t. I is the number of photons absorbed per second, and A is the fraction absorbed by the Co ← L($\pi$*) band.[11] Solution concentrations were adjusted to absorb at least 90% of the incident light, $I_o$.

## Ligand Analysis

Gas chromatographic procedures were used for identification of ligands in photolysis experiments. Large reaction volumes (250 ml) were used in these determinations to allow sufficient free ligand accumulation (approx. 0.1 mmol). A 300 ml photolysis cell was used.[16] The solution was maintained at 7°C by partial immersion in a water bath fitted with a circular glass tube through which cooling water from a Lauda water bath was circulated. This procedure minimized thermally accelerated ligand aquation during lengthy irradiation times (10-30 hr) required for buildup of free ligand concentration.

# CHAPTER 4

# RESULTS

## Kinetic Studies

Reduction of 4-vinylpyridinepentaammineruthenium(III) ion $A_5Ru(III)vp$ by cuprous ion results in "saturation" kinetic behavior; i.e., a change from second to first order with increasing concentrations of reactants.[12] Rate data for three temperatures are shown in Figure 3. Rate constants for individual concentration pairs are tabulated in Table 7. The rate data can be explained by strong association of the reactant ions and can be fitted to Scheme III.

Scheme III.

$$\begin{tikzcd}
Cu(I) + A_5Ru(III)vp \arrow[rr, shift left, "k_f"] \arrow[dr, "k_b"'] & & A_5Ru(III)vp\cdot Cu(I) \arrow[ll, shift left, "k_r"] \arrow[dl, "k_a"] \\
& Cu(II) + A_5Ru(II)vp &
\end{tikzcd}$$

The observed rate constant, $k_o$, is given by $k_o = k'/(1 + 1/K\ A_5Ru(III))$ for $[Ru(III)] >> [Cu(I)]$, where $K = k_f/k_r$ and $k' = k_a + k_b/K$; a symmetrical relationship holds for $[Cu(I)] >> [Ru(III)]$. The parameters K and k' were determined from double reciprocal plots using the expression: $1/k_o = 1/k' + 1/k'K[Ru(II)]$, where plotting

## TABLE 7

Rate Data for $A_5Ru(III)vp + Cu(I) \rightleftharpoons A_5Ru(II)vp + Cu(II)$[a]

| Temp. (°C) | $10^4 \cdot$ $[A_5Ru(III)vp]$ (M) | $10^4 \cdot$ $[Cu(I)]$ (M) | $10^2 \cdot$ $k_o$ (sec$^{-1}$)[b] |
|---|---|---|---|
| 4 | 0.1 | 1.0 | 1.26 ± 0.15 |
| | 1.8 | 0.3 | 1.89 ± 0.60 |
| | 0.2 | 2.0 | 1.69 ± 0.15 |
| | 4.0 | 0.4 | 2.13 ± 0.00 |
| | 4.5 | 0.45 | 2.77 ± 0.10 |
| | 0.6 | 6.0 | 2.60 ± 0.11 |
| | 0.77 | 7.0 | 2.68 ± 0.16 |
| | 7.0 | 0.7 | 2.77 ± 0.10 |
| | 7.7 | 0.7 | 2.80 ± 0.01 |
| | 9.0 | 0.9 | 2.66 ± 0.10 |
| | 16.0 | 1.1 | 2.80 ± 0.20 |
| | 2.0 | 20.0 | 2.91 ± 0.10 |
| | 2.78 | 30.0 | 3.08 ± 0.30 |
| 23 | 4.0 | 1.25 | 8.0 ± 0.30 |
| | 5.0 | 2.0 | 9.3 ± 0.95 |
| | 6.5 | 1.85 | 9.7 ± 0.20 |
| | 7.8 | 2.0 | 12.3 ± 0.50 |
| | 9.0 | 2.25 | 12.8 ± 0.50 |
| | 13.0 | 2.6 | 14.0 ± 0.60 |
| | 26.0 | 5.2 | 18.9 ± 1.50 |
| 41 | 3.6 | 1.2 | 23.1 ± 0.00 |
| | 4.0 | 1.0 | 22.5 ± 0.01 |
| | 4.18 | 1.0 | 26.0 ± 0.29 |
| | 5.0 | 1.25 | 18.9 ± 0.07 |
| | 5.25 | 1.75 | 27.0 ± 0.30 |
| | 6.0 | 2.0 | 27.0 ± 0.30 |
| | 7.35 | 2.0 | 41.6 ± 0.02 |
| | 8.35 | 2.09 | 40. ± 0.22 |
| | 8.36 | 2.0 | 38.5 ± 0.20 |
| | 9.75 | 2.5 | 52.1 ± 0.57 |
| | 5.0 | 10.0 | 26.8 ± 0.24 |
| | 16.0 | 4.0 | 51.3 ± 0.31 |
| | 30.0 | 10.0 | 77.0 ± 0.00 |
| | 33.5 | 16.0 | 74.7 ± 0.17 |
| | 35.0 | 7.0 | 76.0 ± 0.45 |
| | 39.0 | 10.0 | 80.0 ± 0.60 |

---

[a] In 0.1 M HTFA, $[Cu(II)]_o = 1 \times 10^{-4}$, $[Cu(III)] = [Cu(I)]_o$.

[b] All entries are the average results of three or more individual determinations.

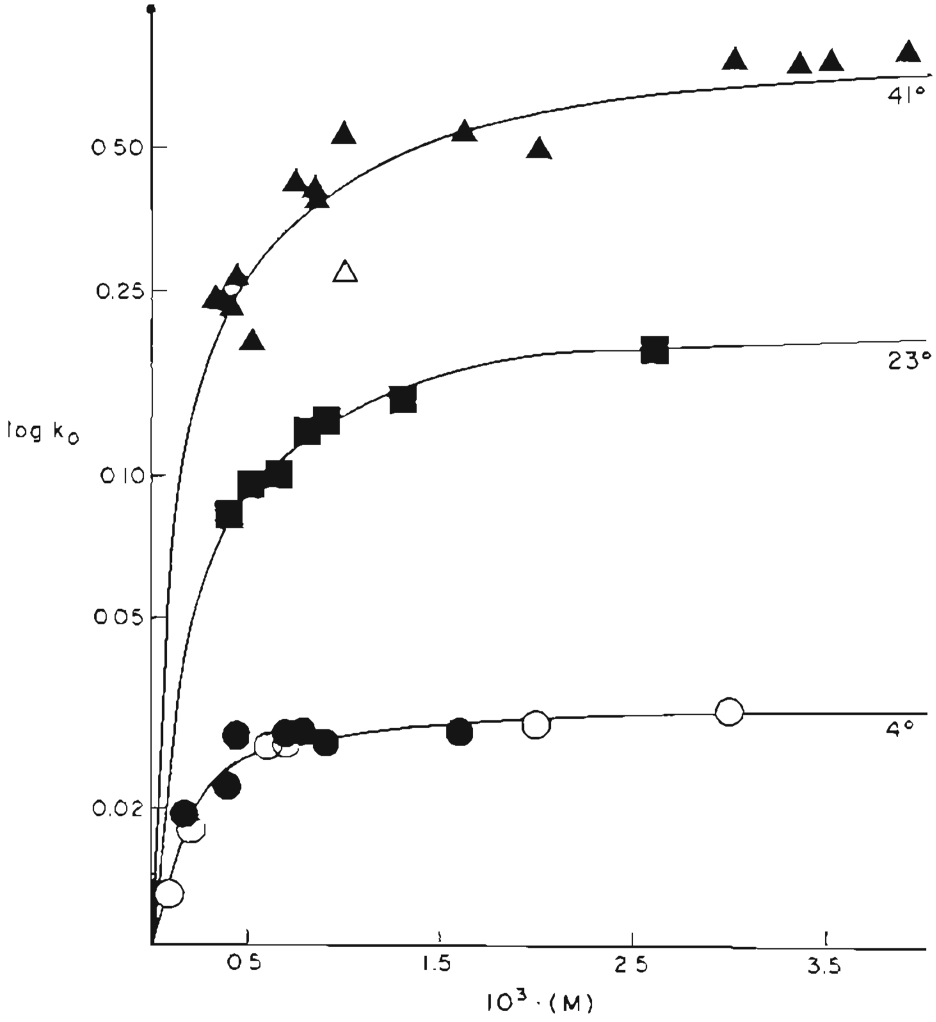

Figure 3. Cu(I) reduction of $A_5Ru(III)vp$. Conditions are those listed in Table 6. The solid lines represent the theoretical $k_o$ value calculated for the mechanism given in Scheme III using the best fit values of K and k' (Table 10). Open points are [Cu(I)] in excess, closed points are [$A_5Ru(III)$ vp] in excess.

the reciprocal of the observed rate vs. the inverse of the concentration gives the intercept 1/k'. The equilibrium constant, K, is then obtainable from the slope, 1/k'K. The parameters K and k' were determined at three different temperatures from plots of $k_o^{-1}$ vs. $[Ru(NH_3)_5vp]^{-1}$ which were linear (Figures 4, 5 and 6).

Reduction of other $(NH_3)_5Ru(III)py$ ions by Cu(I) and Cu(I)-allylalcohol-π-complex ion exhibited second order kinetics over the experimental concentration range: $d[Ru(II)]/dt = k[Cu(I)][Ru(III)]$. Conditions are given in Tables 8 and 9. Plots of data are represented by Figures 7, 8 and 9 for the $A_5Ru(III)etpy$ and $A_5Ru(III)py$ system, respectively.

The reduction of the pyridinepentaammineruthenium complexes was well behaved. Reactant concentrations were varied over (10-400)-fold ranges and rate constants were the same for either reactant held in excess ($Ru(III)/Cu(I) \doteq 0.1\text{-}10$); no systematic deviation from the rate laws was apparent. Kinetic plots were linear to better than 2.5 half-lives. For runs with Ru(III) in excess, Ru(II) product concentrations were 90-100% of the stoichiometric equivalents of added Cu(I) as calculated from the total absorbancy changes. Therefore, the overall redox stoichiometries are:

$$Cu(I) + Ru(III) \rightarrow Cu(II) + Ru(II).$$

The reverse reaction comprising reduction of cupric ion by $A_5Ru(II)vp$ ion was studied in the presence of saturating $O_2$, which oxidizes Cu(I) formed, driving the reaction to completion (Scheme IV).

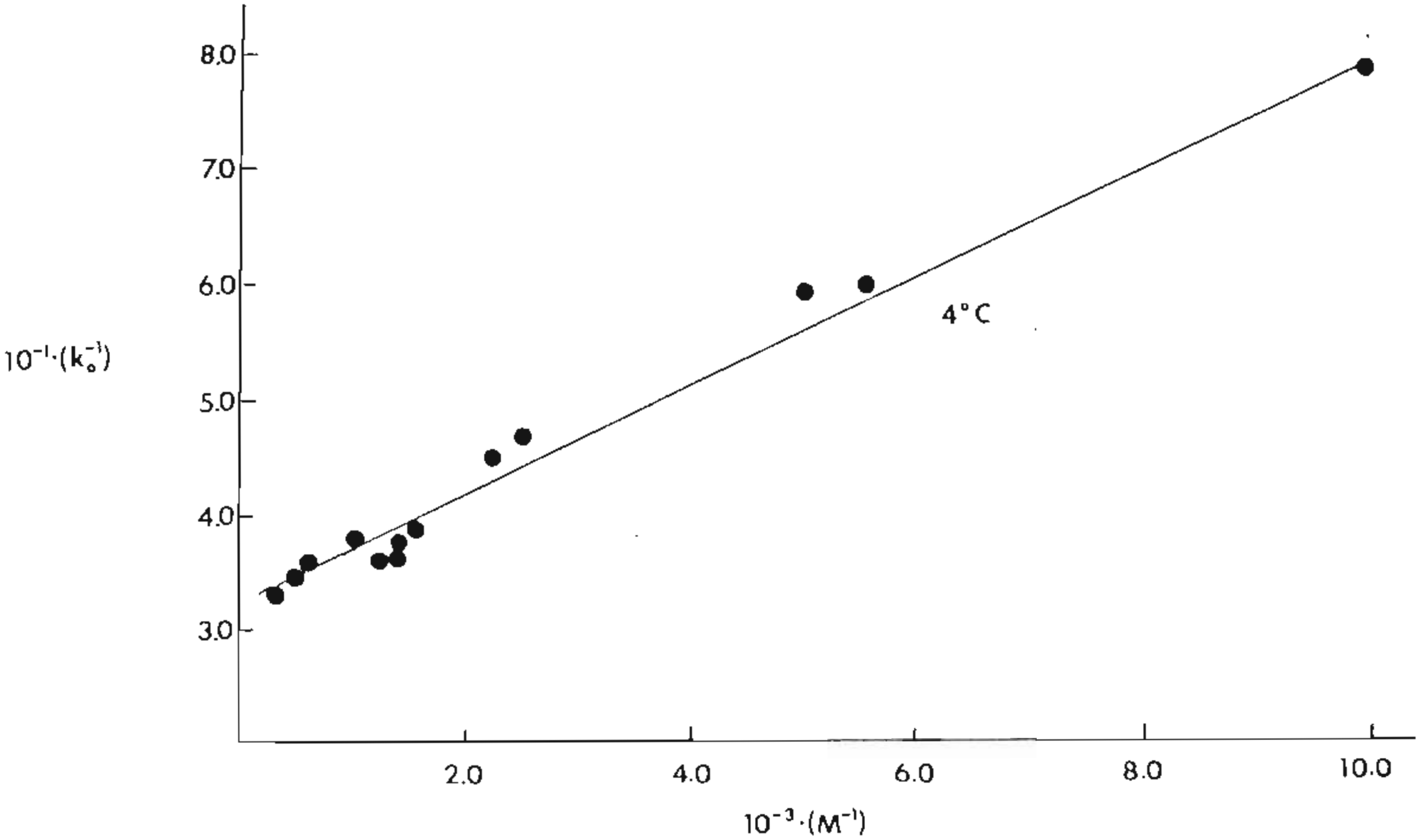

Figure 4. Reciprocal plot for the $A_5$Ru(III)vp-Cu(I) reaction at 4°C. Conditions are those listed in Table 6. The line drawn is from simple linear regression analysis of the data.

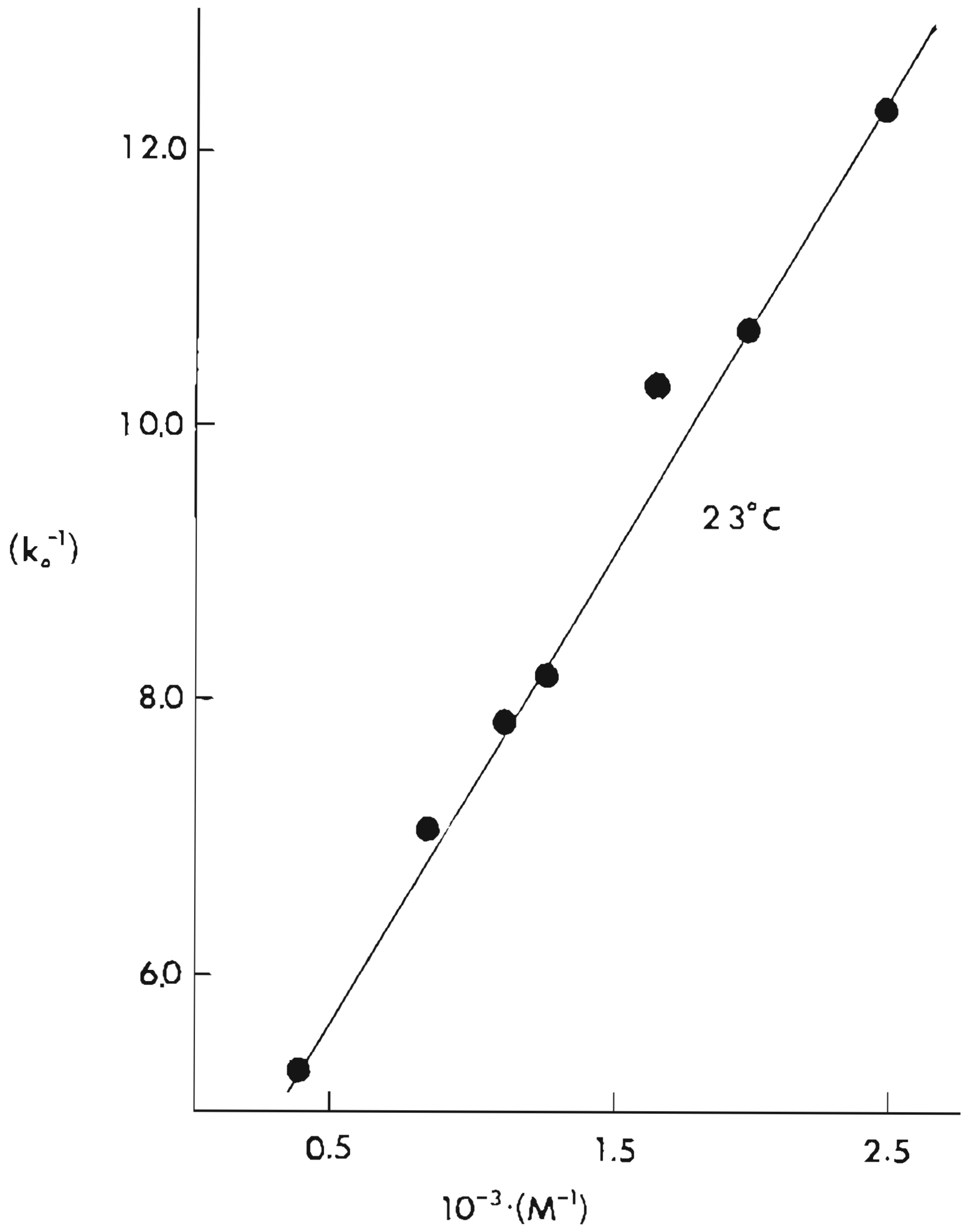

Figure 5. Reciprocal plot for the $A_5Ru(III)vp$-$Cu(I)$ reaction at 23°C. Conditions are those listed in Table 6. The line drawn is from simple linear regression analysis of the data.

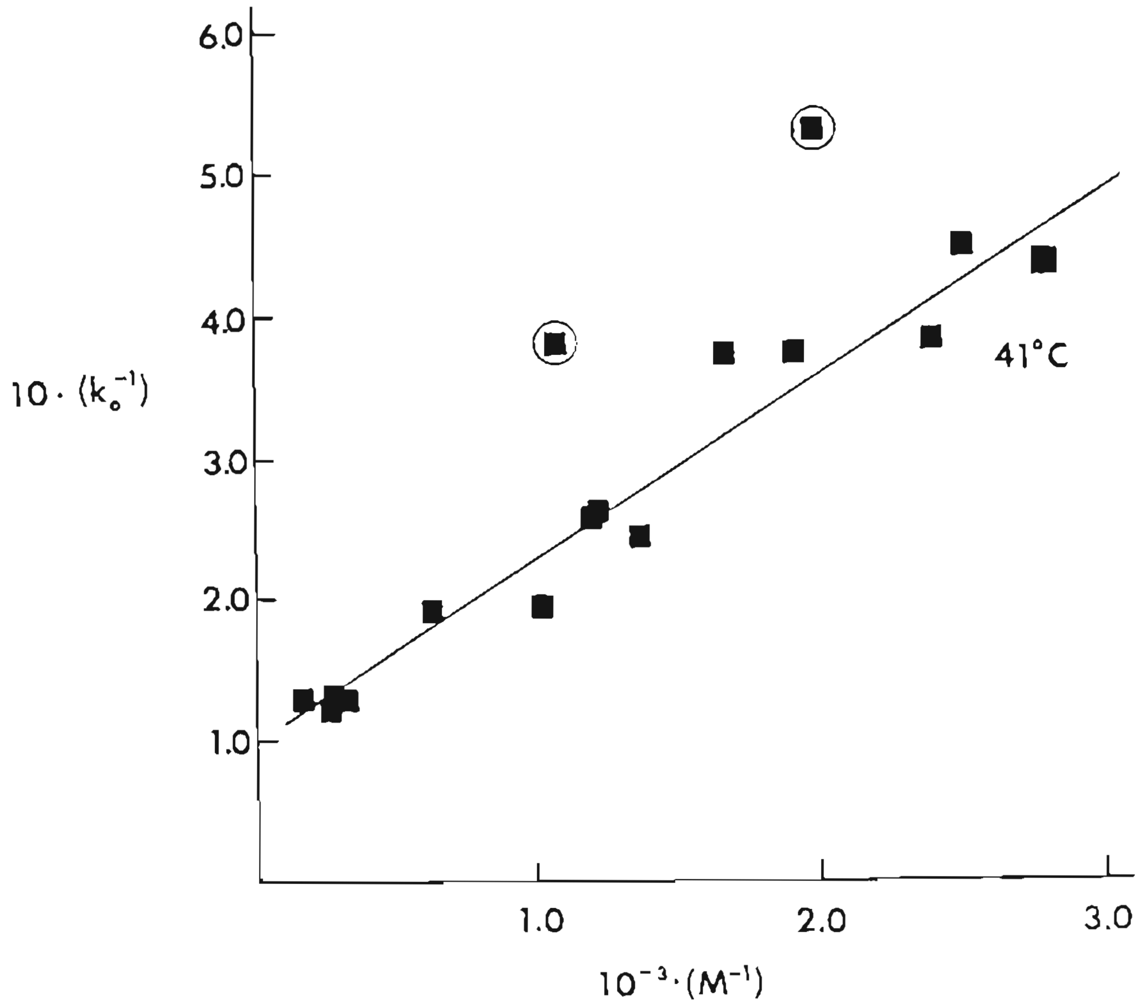

Figure 6. Reciprocal plot for the $A_5Ru(III)vp$-Cu(I) reaction at 41°C. Conditions are those listed in Table 6. The line drawn is from simple linear regression analysis of the data with exclusion of the circled data points.

## TABLE 8

Rate Data for $A_5Ru(III)etpy + Cu(I) \rightleftharpoons A_5Ru(II)etpy + Cu(II)$[a]

| Temp. (°C) | $10^4 \cdot [Cu(I)]$ (M) | $10^4 \cdot [A_5Ru(III)etpy]$ (M) | $10^3 \cdot k_o$ ($s^{-1}$)[b] | $k_{2nd}$ ($M^{-1}s^{-1}$) |
|---|---|---|---|---|
| 4 | 7 | 0.7 | 1.98 ± 0.24 | 2.85 |
| | 8 | 0.8 | 1.99 ± 0.06 | 2.48 |
| | 4 | 0.4 | 1.46 ± 0.30 | 3.65 |
| | 11.0 | 1.8 | 2.66 ± 0.19 | 2.4 |
| | 14.0 | 1.4 | 3.58 ± 0.27 | 2.55 |
| | 20.0 | 2.0 | 5.01 ± 0.08 | 2.5 |
| 24 | 4 | 0.4 | 2.93 ± 0.26 | 5.1 |
| | 8 | 0.8 | 4.70 ± 0.37 | 5.8 |
| | 12 | 1.2 | 6.82 ± 0.22 | 5.68 |
| | 16 | 1.6 | 8.23 ± 0.17 | 5.14 |
| 41 | 4.0 | 0.4 | 4.95 ± 0.61 | 12.3 |
| | 10.0 | 1.0 | 10.0 ± 1.2 | 10.0 |
| | 1.4 | 14.0 | 19.9 ± 1.4 | 14.2 |
| | 18 | 1.8 | 20.2 ± 1.3 | 11.2 |

[a] In 0.1 M HTFA; other ions present $[Cu(II)] = 1 \times 10^{-4}$ and $[Cr(III)]_o = [Cu(I)]$.

[b] All entries are the results of three or more individual determinations.

TABLE 9

Rate Data for $A_5Ru(III)py + Cu(I)\text{-}\pi\text{-allylalcohol} \rightleftharpoons A_5Ru(II) + Cu(II) + \text{allylalcohol}$[a]

| Temp. (°C) | $10^4 \cdot [Cu(I)]$(M) | $10^3 \cdot [A_5Ru(III)py]$(M) | $10^3 \cdot k_o (s^{-1})$ | $k_{2nd} (n^{-1}s^{-1})$ |
|---|---|---|---|---|
| 4 | 1.0 | 6.4 | $0.53 \pm 0.09$ | 0.083 |
| | 3.5 | 12.6 | $1.27 \pm 0.02$ | 0.10 |
| | 2.5 | 14.3 | $1.85 \pm 0.10$ | 0.13 |
| | 2.5 | 16.2 | $1.70 \pm 0.10$ | 0.11 |
| | 2.5 | 25.0 | $2.25 \pm 0.04$ | 0.11 |
| 24 | 3.0 | 3.0 | $1.28 \pm 0.06$ | 0.43 |
| | 4.0 | 4.5 | $1.49 \pm 0.08$ | 0.33 |
| | 2.5 | 6.0 | $2.28 \pm 0.15$ | 0.38 |
| | 4.0 | 6.0 | $2.53 \pm 0.34$ | 0.42 |
| | 4.0 | 7.7 | $3.46 \pm 0.13$ | 0.45 |
| | 3.0 | 9.0 | $3.40 \pm 0.01$ | 0.37 |
| 47 | 1.0 | 0.50 | $1.67 \pm 0.05$ | 3.35 |
| | 1.0 | 0.75 | $2.76 \pm 0.07$ | 3.68 |
| | 1.0 | 1.0 | $3.74 \pm 0.51$ | 3.71 |
| | 5.0 | 3.5 | $13.5 \pm 0.61$ | 3.85 |
| | 5.0 | 5.0 | $18.9 \pm 1.9$ | 3.79 |

[a] All entries are the result of three or more individual determinations; other species present are $1 \times 10^{-4}$ M Cu(II) and 0.1 M HTFA and [Cr(III)] = [Cu(I)].

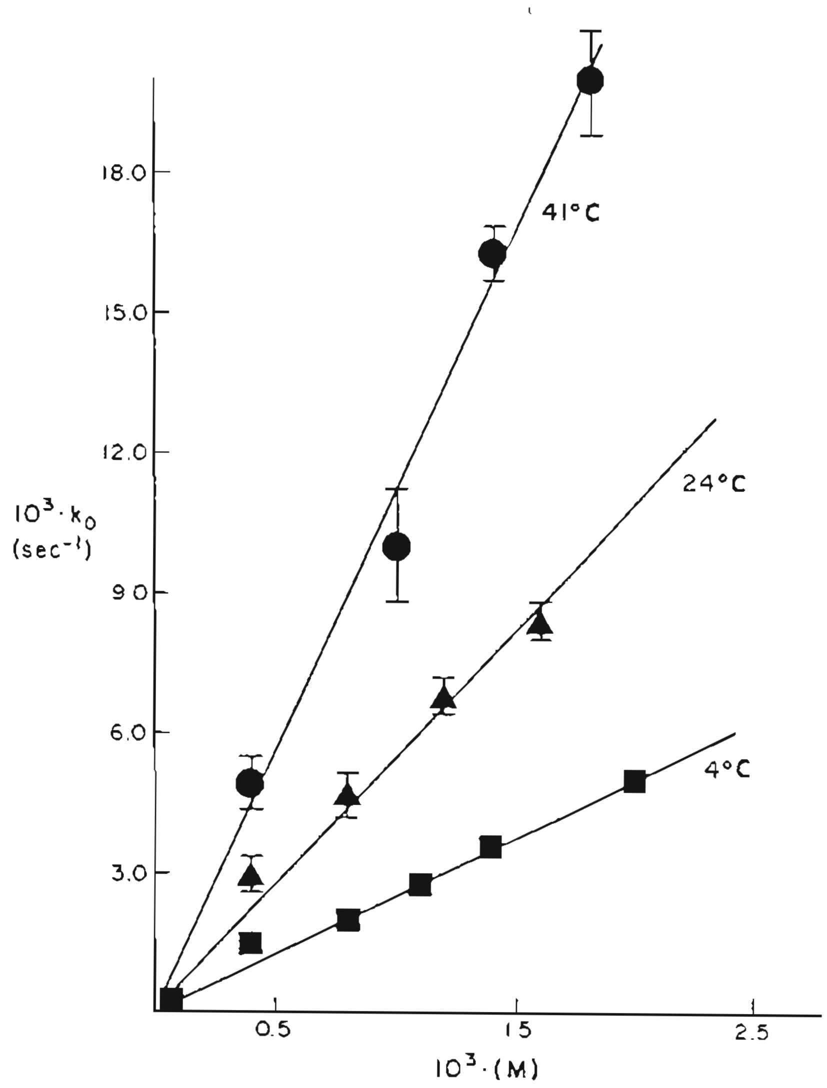

Figure 7. Cu(I) reduction of $A_5Ru(III)$etpy. Conditions are those listed in Table 7. Solid lines were drawn using simple linear regression analysis of the data and constrained to go through the origin.

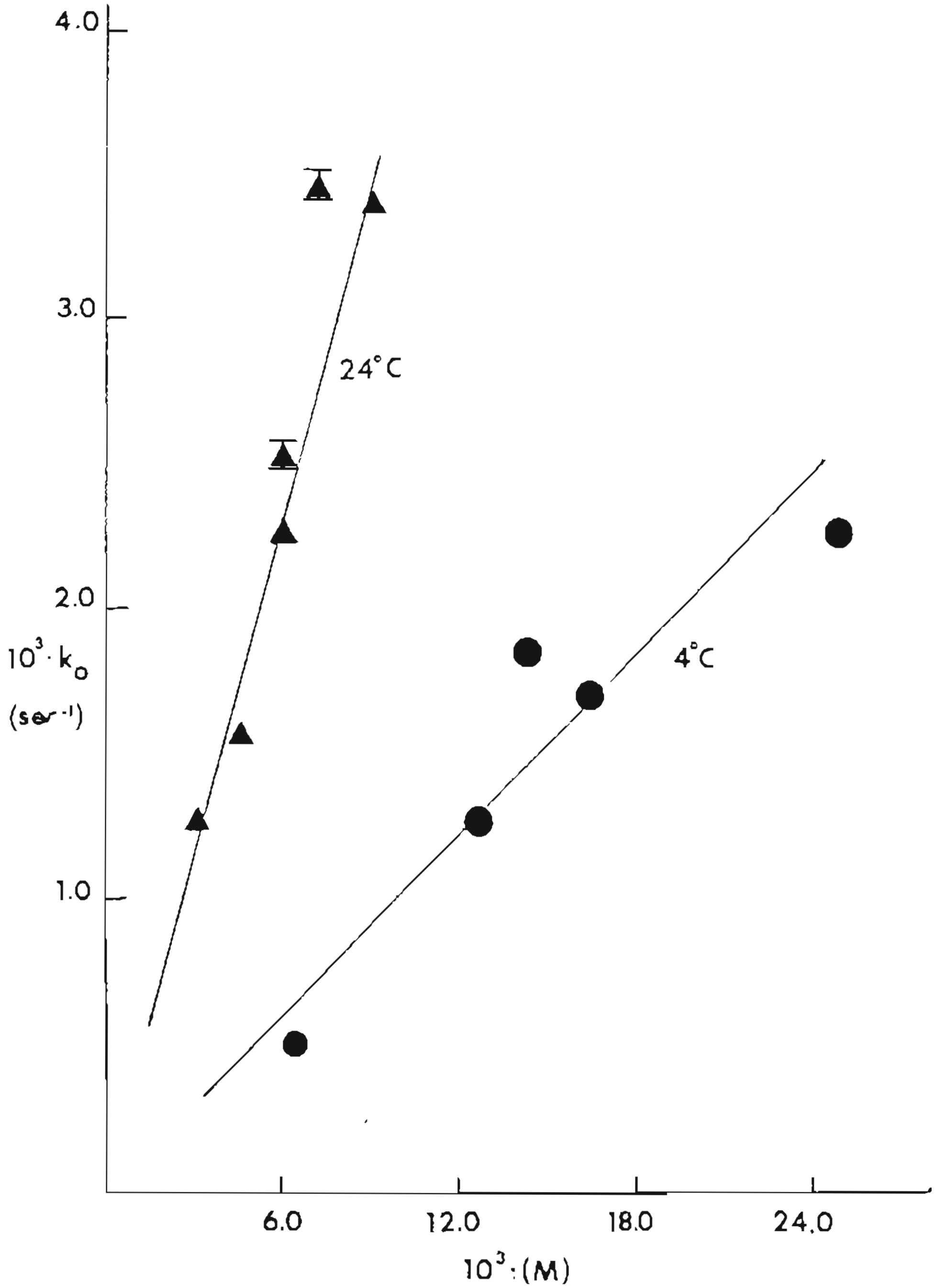

Figure 8. Cu(I)-π-allylalcohol reduction of $A_5Ru(III)py$ at 4°C and 24°C. Conditions are those listed in Table 8. The solid line was drawn using simple linear regression analysis of the data and constrained to go through the origin.

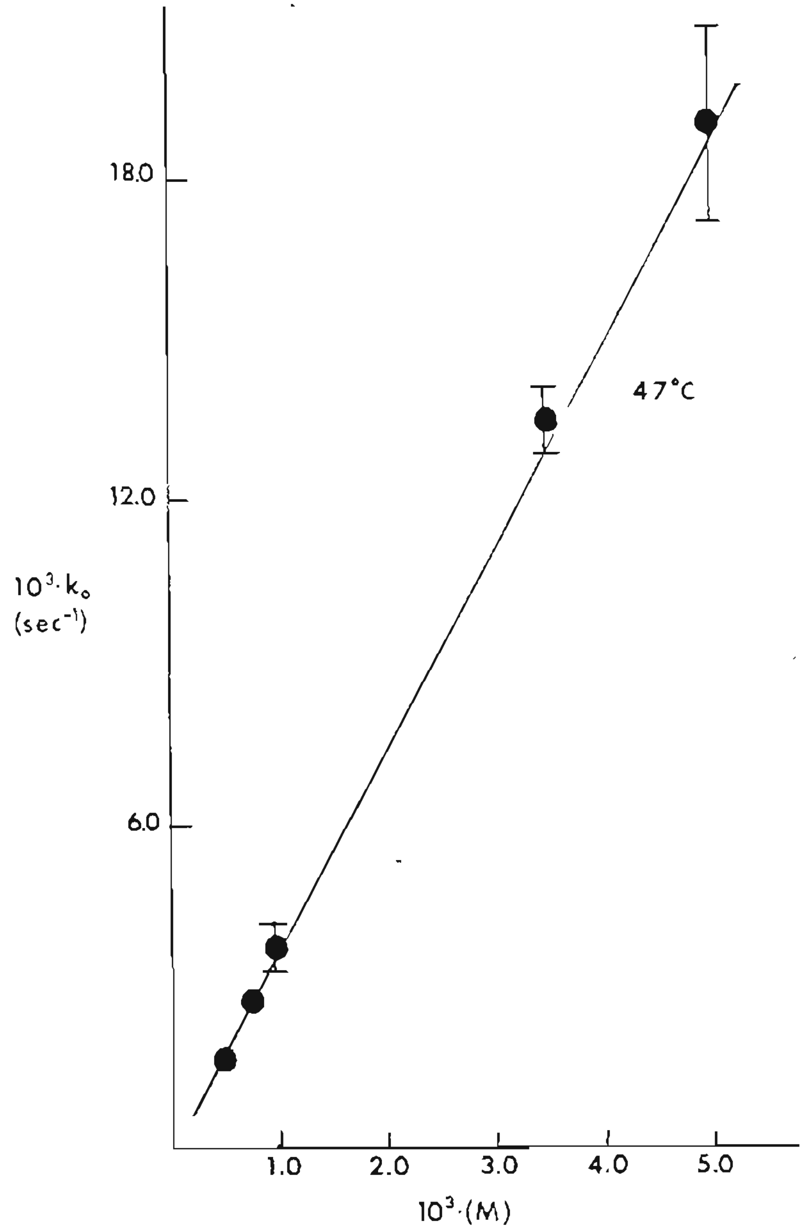

Figure 9. Cu(I)-π-allylalcohol reduction of $A_5$Ru(III)py at 47°C. Conditions are those listed in Table 9. The solid line was drawn using simple linear regression analysis of the data and contrained to go through the origin.

Scheme IV.

$$\mathrm{A_5Ru(II)vp + Cu(II) \underset{k_2}{\overset{k_1}{\rightleftharpoons}} A_5Ru(III)vp + Cu(I)}$$

$$\mathrm{H^+ + Cu(I) + \tfrac{1}{4}\, O_2 \xrightarrow{k_3} Cu(II) + \tfrac{1}{2}\, H_2O}$$

Step 2 is extremely rapid because $k_3 >> k_2$ electron transfer from $A_4$Ru(II)vp to Cu(II) is rate limiting. This reaction was studied over the concentration ranges [Cu(II)] = 1.0-50 mM, [Ru(II)] = 0.5-1.0 mM (Table 10) (results are presented in Figures 10, 11 and 12) and followed the rate law $-d[A_5Ru(III)vp]/dt = k[A_5Ru(II)vp][Cu(II)]$. Direct oxidation of $A_5$Ru(II)vp by $O_2$ was studied to determine its contribution to the measured overall rate.[29]

$$\mathrm{A_5Ru(II)vp + H^+ + \tfrac{1}{2}\, O_2 \rightarrow A_5Ru(III)vp + \tfrac{1}{2}\, H_2O_2}$$

With excess $O_2$ the reaction follows pseudo-first order kinetics with $k_{O_2} = 0.64$, 3.2, and $14 \times 10^{-4} s^{-1}$ at 3, 23 and 47°C respectively. Only under high temperature and low Cu(II) concentrations was it necessary to apply this correction, which was at most 15% of the overall rate. A summary of kinetic parameters for Cu(I) → Ru(III) redox reactions is presented in Table 11.

Thermodynamic and activation parameters for the reactions evaluated from their temperature dependencies are given in Table 12. The plots (ln K vs. $T^{-1}$ and ln k'/T vs. $T^{-1}$) were linear and are shown in Figures 13, 14, 15, 16 and 17.

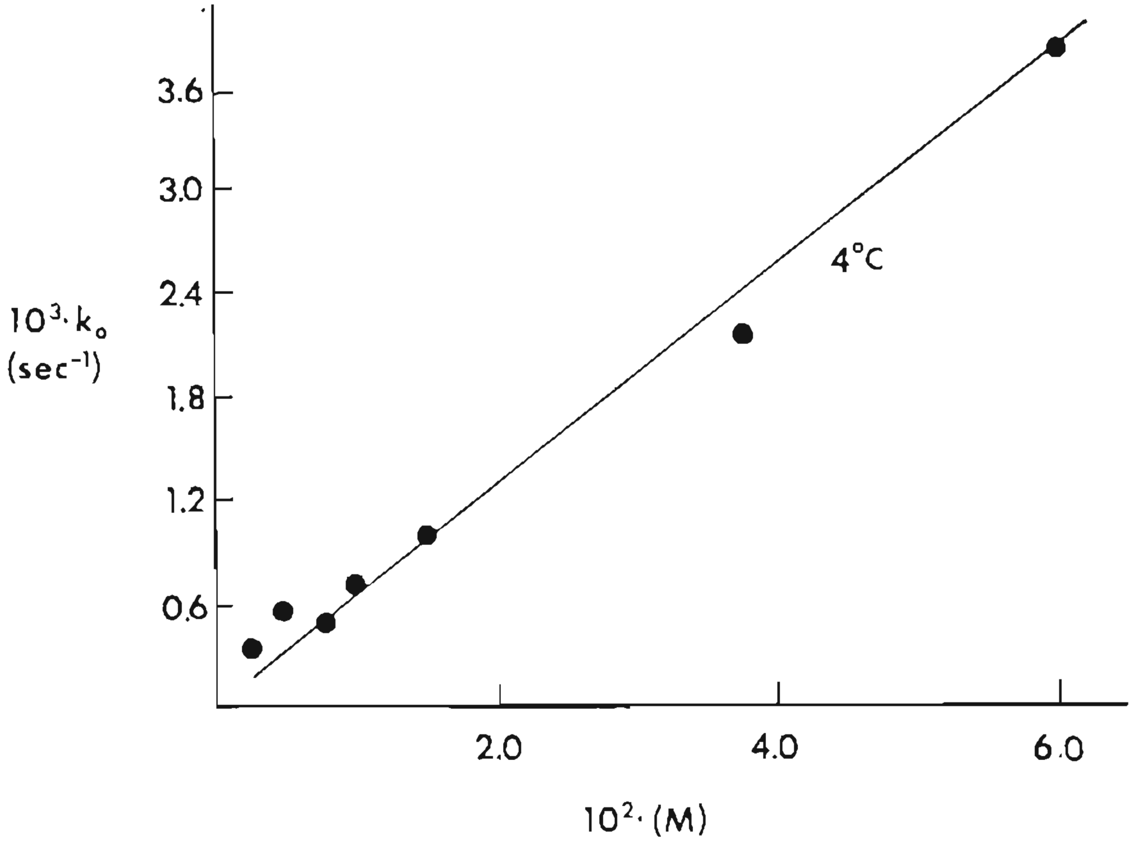

Figure 10. Cu(II) oxidation of $A_5Ru(II)vp$ at 4°C. Conditions are those listed in Table 9. The solid line was drawn using simple linear regression analysis of the data and constrained to go through the origin.

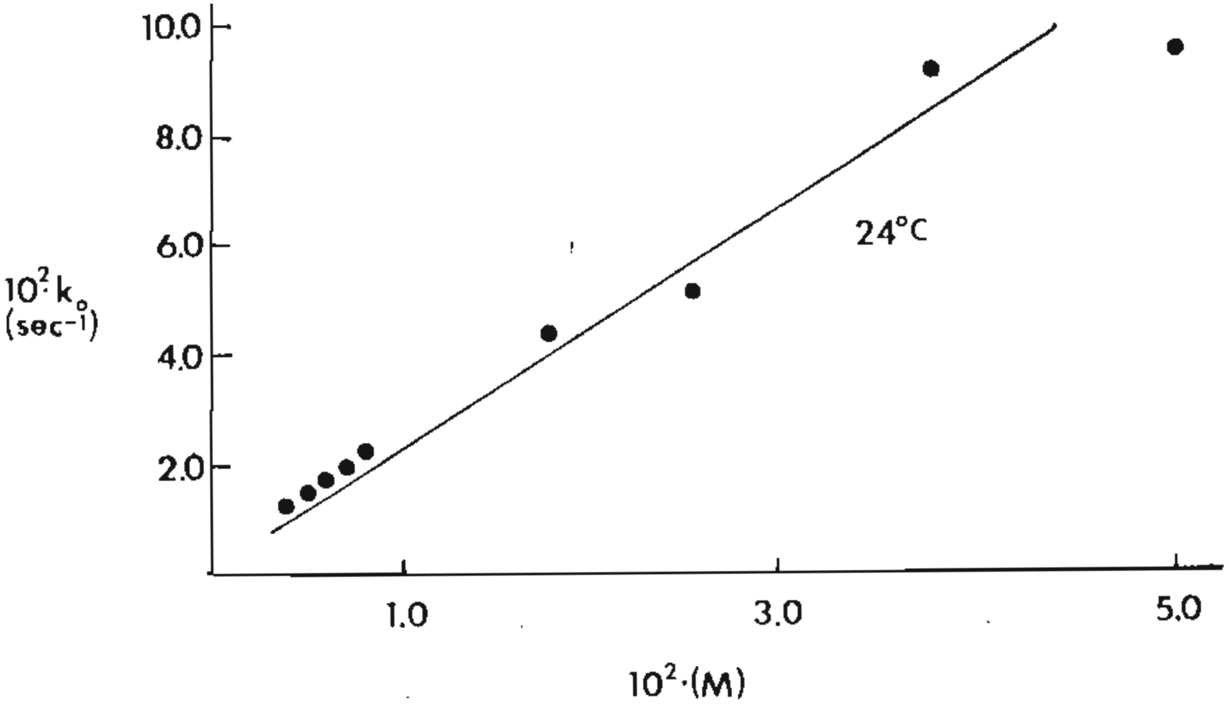

Figure 11. Cu(II) oxidation of $A_5$Ru(II)vp at 24°C. Conditions are given in Table 9. The solid lines were drawn using simple linear regression analysis of the data and constrained to go through the origin.

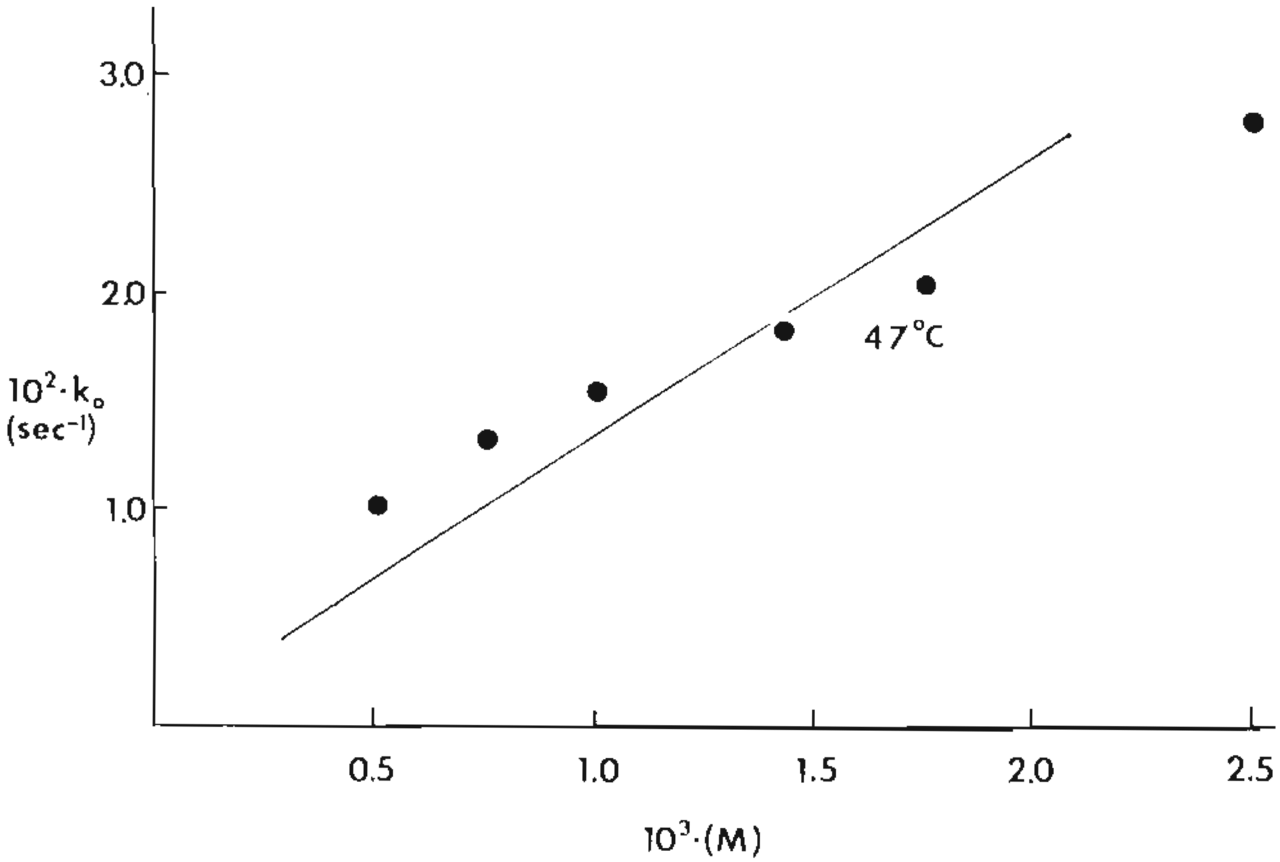

Figure 12. Cu(II) oxidation of $A_5Ru(II)vp$ at 47°C. Conditions are given in Table 9. The solid line was drawn using simple linear regression analysis of the data and constrained to go through the origin.

TABLE 10

Rate Data for $Cu(II) + A_5Ru(II)vp \rightleftharpoons Cu(I) + A_5Ru(III)vp$[a]

| Temp. (°C) | $10^3\cdot$ [Cu(II)](M) | $10^4\cdot$ $[A_5Ru(II)vp]$(M) | $10^2\cdot$ $k_o$(sec$^{-1}$)[b] | $k_{2nd}$($M^{-1}s^{-1}$) |
|---|---|---|---|---|
| 4 | 2.5 | 1.0 | 0.370± 0.005 | 1.48 |
| | 5.0 | 0.5 | 0.686± 0.044 | 1.37 |
| | 7.5 | 1.0 | 0.592± 0.015 | 0.78 |
| | 10.0 | 1.0 | 0.670± 0/034 | 0.67 |
| | 15.0 | 1.0 | 0.969± 0.007 | 0.65 |
| | 37.5 | 1.0 | 2.10 ± 0.12 | 0.56 |
| | 60.0 | 1.0 | 3.78 ± 0.13 | 0.63 |
| 24 | 4.0 | 0.8 | 1.26 ± 0.04 | 3.15 |
| | 6.0 | 0.8 | 1.72 ± 0.00 | 2.86 |
| | 7.0 | 1.0 | 1.98 ± 0.02 | 2.83 |
| | 8.0 | 0.8 | 2.20 ± 0.01 | 2.75 |
| | 10.0 | 1.0 | 2.65 ± 0.00 | 2.65 |
| | 17.5 | 1.0 | 4.37 ± 0.60 | 2.44 |
| | 25.0 | 1.0 | 5.01 ± 0.00 | 2.00 |
| | 37.5 | 1.0 | 9.12 ± 0.00 | 2.43 |
| | 50.0 | 1.0 | 9.55 ± 0.22 | 1.91 |
| 47 | 0.50 | 0.5 | 1.02 ± 0.04 | 20.0 |
| | 0.75 | 0.5 | 1.28 ± 0.96 | 16.5 |
| | 1.00 | 0.5 | 1.52 ± 0.16 | 15.2 |
| | 1.45 | 0.5 | 1.82 ± 0.26 | 12.6 |
| | 1.75 | 0.5 | 2.01 ± 0.14 | 11.5 |
| | 2.5 | 0.5 | 2.62 ± 0.20 | 10.4 |

[a] In 0.1 M HTFA in the presence of saturating $O_2$.

[b] Corrected for the $A_5Ru(II)vp + 1/2\ O_2 \rightleftharpoons A_5Ru(III)vp + 1/2\ H_2O_2$ reaction; rates used for this correction are: $14 \times 10^{-4}s^{-1}$, $3.2 \times 10^{-4}s^{-1}$ and $0.64 \times 10^{-4}s^{-1}$ at 47°C, 24°C and 4°C respectively.

## TABLE 11

### Kinetic Summary for Copper-Ruthenium Redox Reactions[a]

| Reactants | T (°C) | $k^b$ | |
|---|---|---|---|
| $A_5Ru(II)vp$, Cu(I) | 4 | $10^{-3}\cdot K_a = 6.2 \pm .5$ | $k' = 0.032 \pm .006$ |
| | 23 | 1.3 ± .3 | 0.24 ± .015 |
| | 41 | 0.77 ± .11 | 0.94 ± .04 |
| $A_5Ru(III)etpy$, Cu(I)[c] | 4 | 2.6 ± .1 | |
| | 23 | 5.4 ± .3 | |
| | 41 | 11.2 ± .9 | |
| $A_5Ru(III)py$, Cu(I)-π[c,d]<br>Cu(I)-π[c,d] | 4 | 0.10 ± .01 | |
| | 24 | 0.40 ± .04 | |
| | 47 | 3.7 ± .1 | |
| Cu(II), $A_5Ru(II)vp$ | 4 | 0.57 ± .06 | |
| | 24 | 2.3 ± .3 | |
| | 47 | 7.7 ± .3 | |

[a] In 0.1 M TFA.

[b] Units: $k(M^{-1}s^{-1})$; $k_a(M^{-1})$; $k'(s^{-1})$.

[c] $[Cu(II)] = 10^{-4}$ M.

[d] π = allylalcohol, $[CH_2{=}CNCH_2OH] = 5 \times 10^{-3}$ M.

## TABLE 12

### Activation Parameters for the Redox Reactions[a]

| Reactants | $\Delta H^{\ddagger}$ (kcal/mol) | $\Delta S^{\ddagger}$[b] (e.u.) |
|---|---|---|
| $A_5Ru(II)vp$, $Cu(I)$ | $(-9.7 \pm 1.7, 15.1 \pm 0.2)$[c] | $(-18 \pm 6, -10 \pm 4)$[d] |
| $A_5Ru(II)etpy$, $Cu(I)$ | $5.5 \pm 0.5$ | $-36 \pm 3$ |
| $A_5Ru(III)py$, $Cu(I)$-$\pi$ | $14.6 \pm 1.4$ | $-11 \pm 5$ |
| $Cu(II)$, $A_5Ru(II)vp$ | $10.2 \pm 0.1$ | $-22 \pm 1$ |

[a] In 0.1 M TFA.

[b] At 23°C.

[c] $(\Delta H_K, \Delta H^{\ddagger}_{k'})$.

[d] $(\Delta S_K, \Delta S^{\ddagger}_{k'})$.

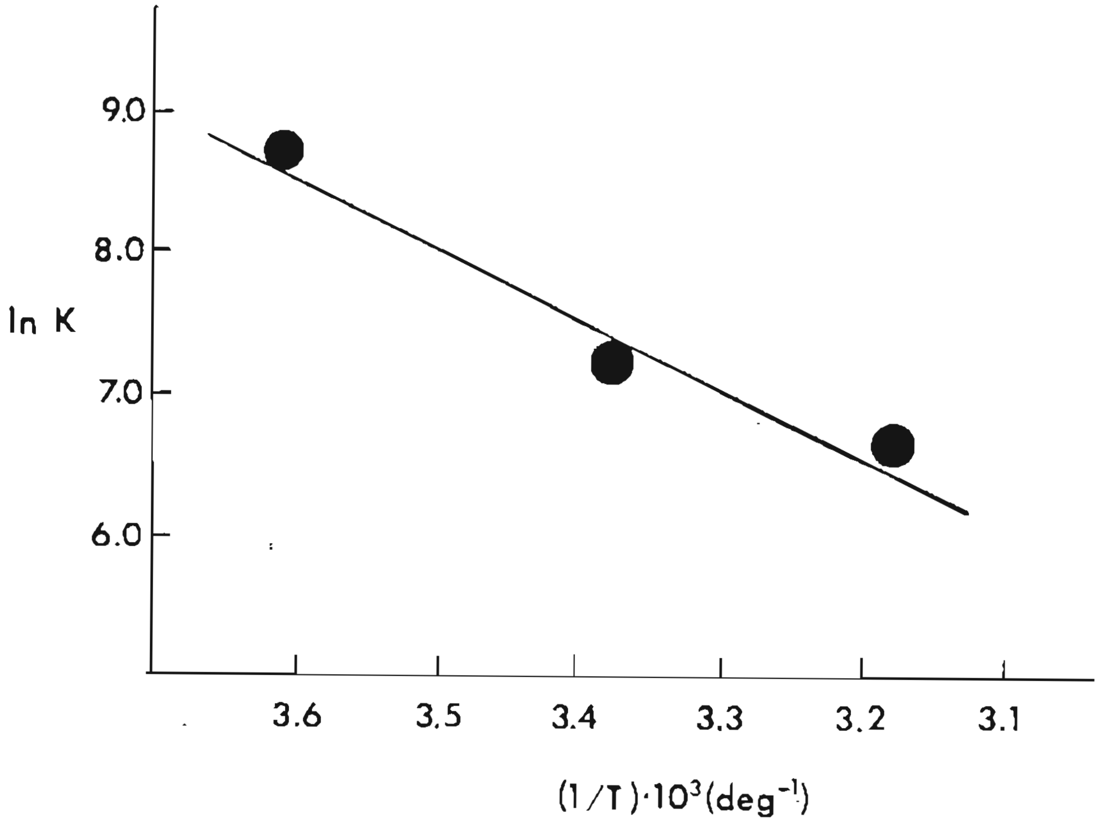

Figure 13. Eyring plot of equilibrium constants for $A_5Ru(III)vp-Cu(I)$ ion association. The line is drawn from simple linear regression analysis of the data.

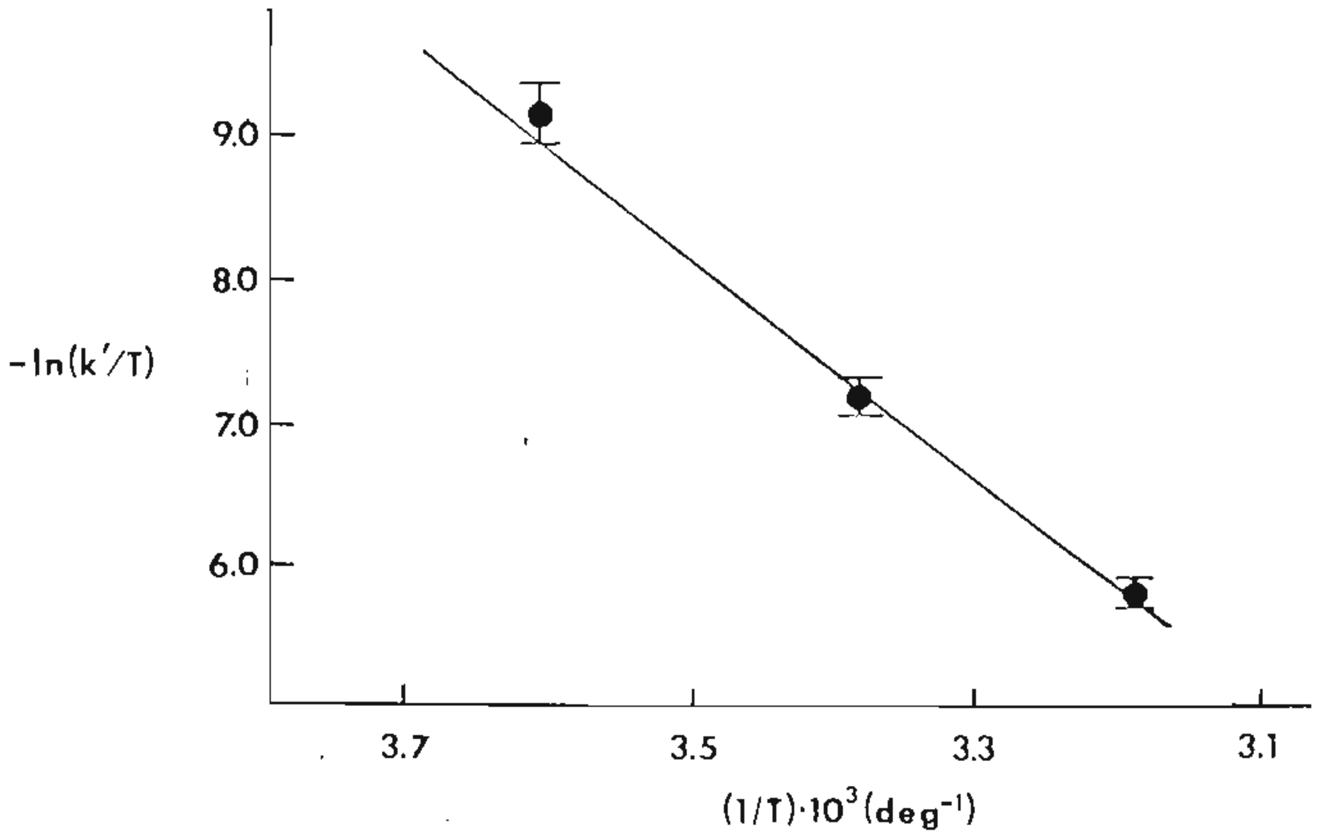

Figure 14. Eyring plot of kinetic data for electron transfer between $A_5Ru(III)vp$ and Cu(I) ion reaction. The line is drawn from simple linear regression analysis of the data.

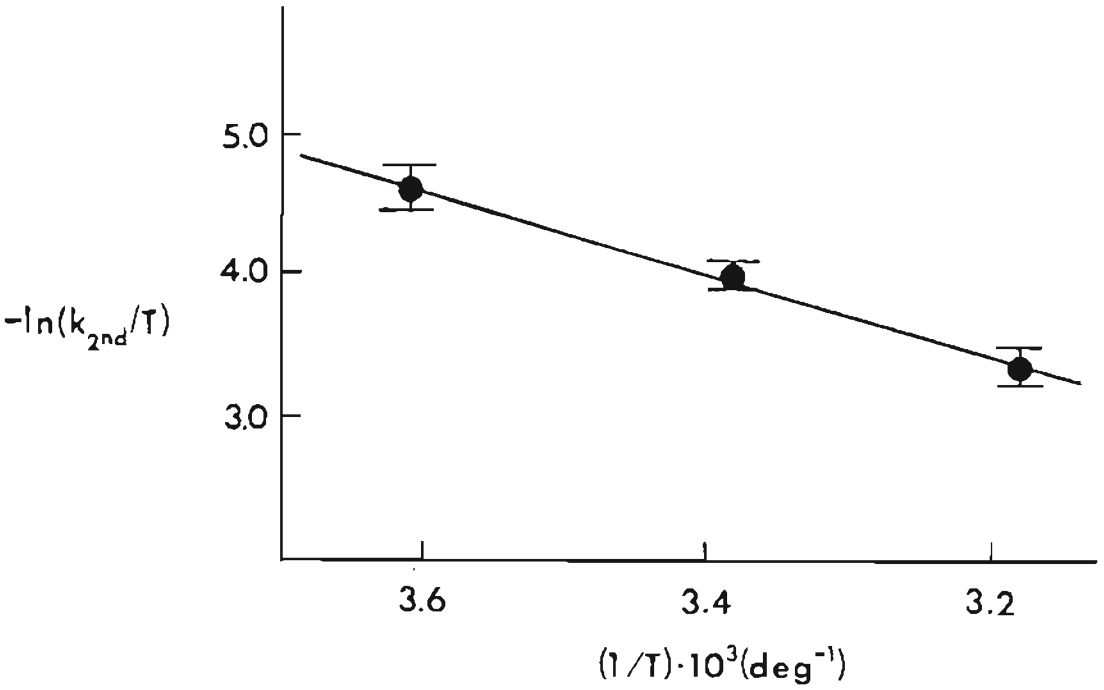

Figure 15. Eyring plot of kinetic data for the reaction of $A_5Ru(III)$etpy-Cu(I) ions reaction. The line is drawn from simple linear regression analysis of the data.

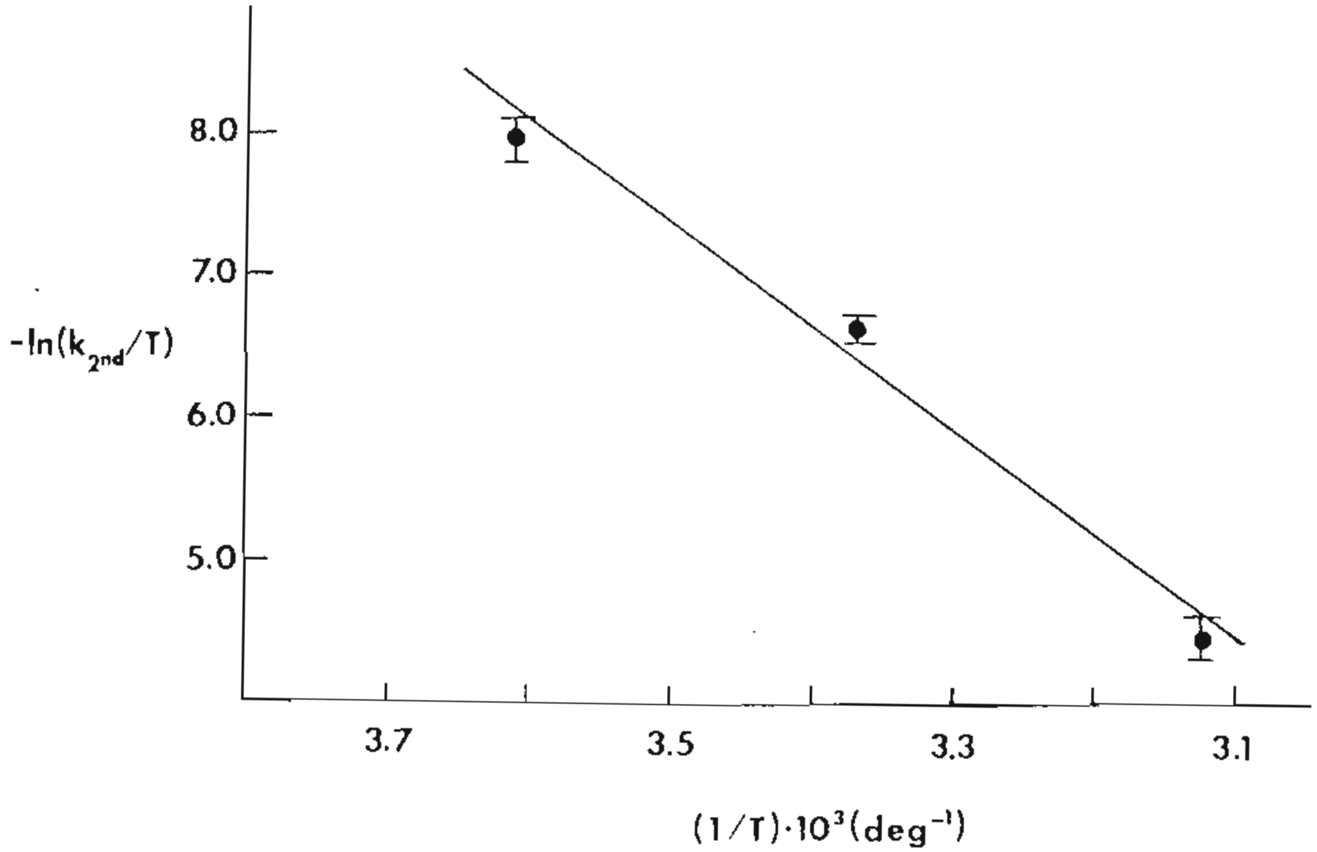

Figure 16. Eyring plot for the $A_5Ru(III)py$-Cu(I)-π-allylalcohol reaction. The line drawn is from simple linear regression analysis of the data.

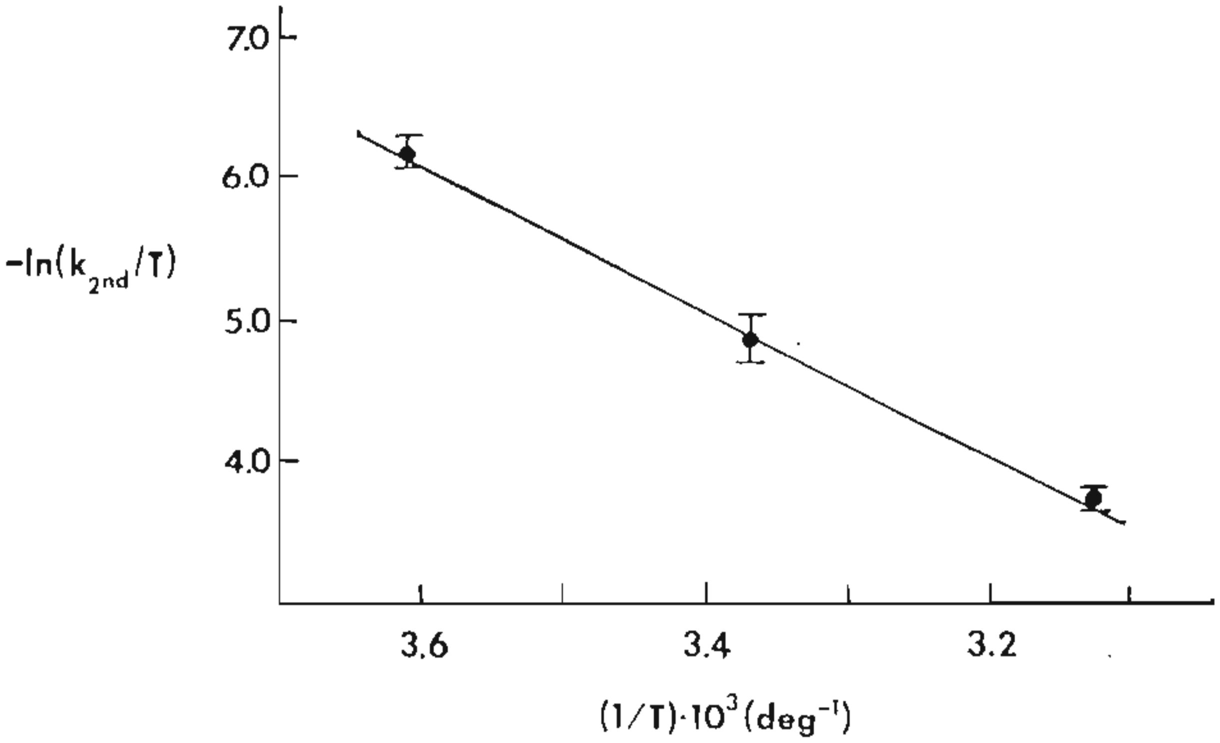

Figure 17. Eyring plot for the $A_5$Ru(II)vp-Cu(II) ions reaction. The line is drawn from simple linear regression analysis of the data.

## Redox Equilibria for the $A_5$Ru(III)-4-vinylpyridine-Cu(I) Reaction

The half-wave reduction potential ($E_{\frac{1}{2}}$) for the Ru(III) ion in 0.1 M HTFA was calculated from the cyclic voltamographic curve to be $(E_{p,a} - E_{p,c})/2$ = 302 mV vs. NHE at 23°C. A similar value has been reported for the $A_5$Ru-pyridine$^{3+/2+}$ redox couple.[30] Peak-to-peak separation was larger ($\Delta E_p \approx 80$ mV) than expected for a reversible process, but was independent of scan rates of 10 to 200 mVs$^{-1}$. Other pyridine-containing ruthenium complexes have shown similar behavior and reasons for the anomalous peak separation have been suggested;[31] typically peak separation should be $\Delta E_p = 58$ mV.[32] As expected for a one-electron process, anodic to cathodic peak current ratios were approximately unity. Figure 18 represents the cyclic voltamograph.

Approximating $E_{\frac{1}{2}} \approx E_r{}^\circ$ for the $A_5$Ru-vp$^{3+/2+}$ couple and using $E_r{}^\circ$ = 153 mV for Cu$^{2+/+}$ the equilibrium constant for the reaction calculated from thermodynamic data is K = [Ru(II)][Cu(II)]/[Ru(III)][Cu(I)] = 344 and from rate data (Table 11) K = 186, the values being in reasonable agreement.

## Difference Absorption Measurement of the $A_5$Ru(III)vp-Cu(I) Binuclear Ion

The reaction presented in Scheme III is reversible and the intermediate binuclear complex should be amenable to study under high Cu(II)/Cu(I) concentration ratios. An absorption spectrum for the intermediate should be attainable if the strong absorbance of the

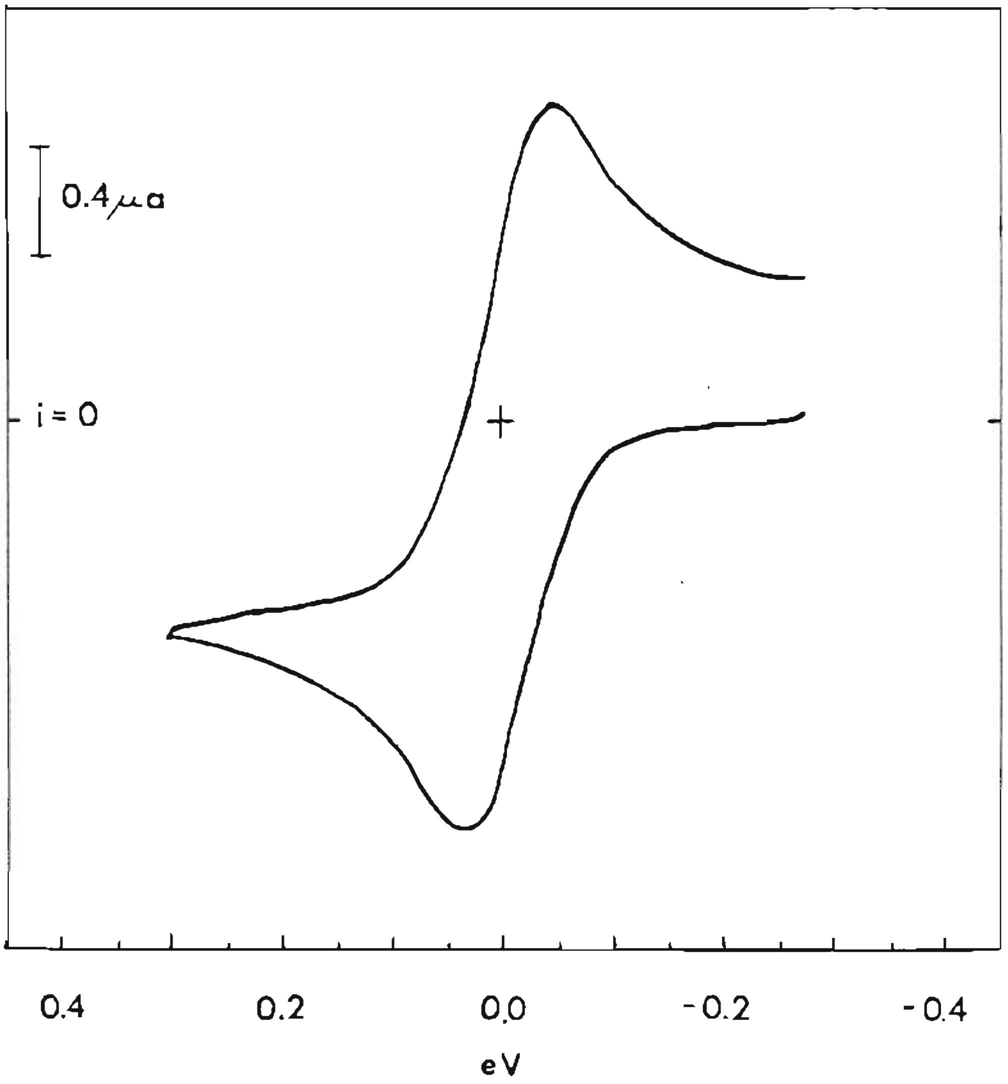

Figure 18. Cyclic voltamograph of $A_5Ru$ vinylpyridine$^{3+/2+}$ couple. Conditions given in text.

$A_5Ru(II)vp$ production can be overcome. Just such a spectrum has been obtained (Figure 19) using the method of difference absorption spectroscopy. Under conditions outlined in the figure which compensate for reactant absorbances there appears both a new u.v. band indicative of Cu(I)-olefin π complexation ($\varepsilon_{363} = 2.2 \times 10^3\ M^{-1}cm^{-1}$) and a rather broad band in the visible with an absorbance maximum at 505 nm and $\varepsilon = 290$. This band cannot be attributed to any of the reactant ions; the spectral properties suggest that the band may be due to intervalence charge transfer from Cu(I) to Ru(III).[33] This experiment has been repeated several times with essentially the same results. Oxygenation of the Cu(I)-containing cells causes the spectrum to return nearly to the baseline absorbance.

### Quantum Yields for Photoinitiated Electron Transfer in $A_5Co(III)$-Cu(I) Binuclear Ions

Irradiation of the Cu(I) → olefin (π*)-charge transfer band results in photodecomposition of cobalt(III)-copper(I) binuclear ions. Quantum yields for the various alkylamine and alkylpyridine ligands are given in Tables 13 and 14 respectively. Values recorded are derived from equation 3 (page 35). Error limits are the average deviation from mean values. Quantum yields for the alkylamine ligands were independent of reactant ion concentrations over the ranges $(A_5Co(III)L)_{total} = 0.5 - 5.0 \times 10^3$ M, $Cu(I)_{total} = 0.25 - 2.5 \times 10^{-3}$ M with Co(III)/Cu(I)) = 2 - 20 and were independent of

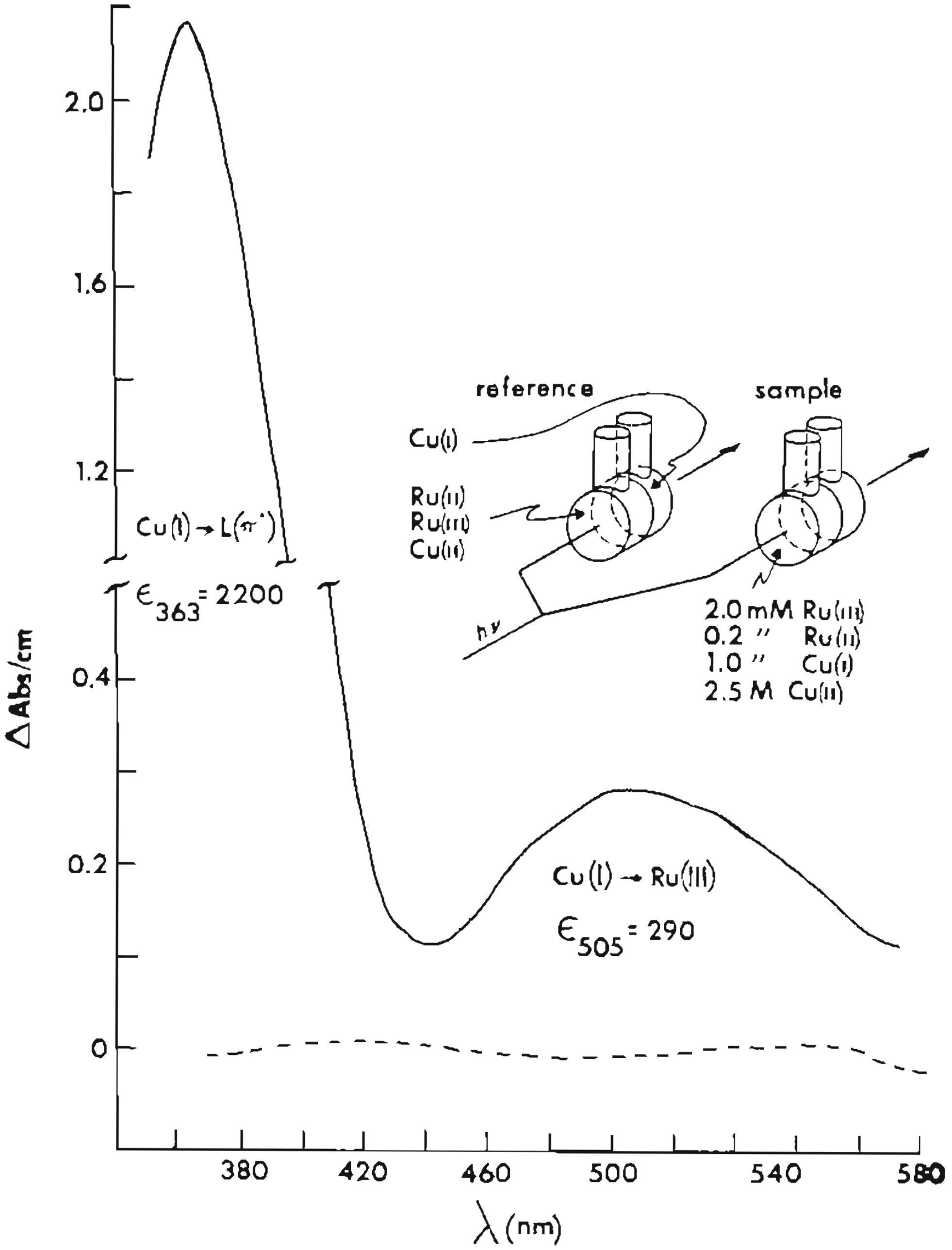

Figure 19. Absorption spectrum of the $A_5Ru(III)vp\text{-}Cu(I)$ ion in 0.1 M HTFA at 23°C. Upper trace: difference spectrum arising from Cu(I)-Ru(III) ion association; lower trace: before Cu(I) addition to the optical cells.

TABLE 13

Quantum Yields for Photoinitiated Electron Transfer in $A_5Co(III)L$-$Cu(I)$ Aminoalkene Binuclear Ions[a]

| Ligand(L) | Irradiation wavelength (nm) | $\Phi$[b] |
|---|---|---|
| $NH_2CH_2CH{=}CH_2$ | 300 | 0.65 ± 0.06(4)[c] |
| $NH_2(CH_2)_2CH{=}CH_2$ | 290 | 0.57 ± 0.09(8)[c] |
| $NH_2(CH_2)_3CH{=}CH_2$ | 306 | 0.34 ± 0.03(7) |
| $NH_2(CH_2)_4CH{=}CH_2$ | 306 | 0.24 ± 0.04(8) |
| $NH_2(CH_2)_6CH{=}CH_2$ | 306 | 0.03 ± 0.01(8) |
| $NH_2(CH_2)_8CH{=}CH_2$ | 306 | < 0.005 |
| 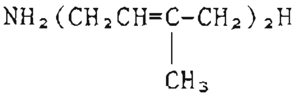 $NH_2(CH_2CH{=}C(CH_3){-}CH_2)_2H$ | 306 | 0.80 ± 0.10(10)<br>0.67 ± 0.04(6) (25% ethanol)<br>0.50 ± 0.02(3) (83% ethanol) |
| 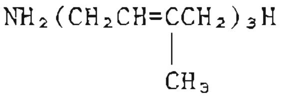 $NH_2(CH_2CH{=}C(CH_3)CH_2)_3H$ | 306 | 0.91 ± 0.06(5)<br>0.51 ± 0.05(4) (50% ethanol)<br>0.33 ± 0.05(3) (90% ethanol) |

[a] In 0.1 M perchloric acid, ambient temperature. Solutions contained in addition 0.015 M Cu(II); $[Cr(III)] = [Cu(I)]_0$.

[b] Number of individual runs given in parentheses; error limits are average deviations from mean values.

[c] From ref. 16.

## TABLE 14

## Quantum Yields for Photoinitiated Electron Transfer in $A_5Co(III)L$-Cu(I) Alkylpyridine Binuclear Ions[a]

| Ligand(L) | Irradiation wavelength (nm) | $\phi$[b] |
|---|---|---|
| $NC_5H_4(CH_2)_2CH{=}CH_2$ | 306 | 0.15 ± 0.043(8) |
| $NC_5H_4(CH_2)_3CH{=}CH_2$ | 306 | 0.10 ± 0.04(8) |
| $NC_5H_4(CH_2)_4CH{=}CH_2$ | 306 | 0.05 ± 0.07(6) |
| $NC_5H_4(CH_2)_5CH{=}CH_2$ | 306 | < 0.005(6) |
| $NC_5H_4(CH_2)_7CH{=}CH_2$ | 306 | < 0.005(6) |
| $NC_5H_4(CH_2)_9CH{=}CH_2$ | 306 | < 0.005(6) |
| 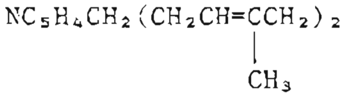 $NC_5H_4CH_2(CH_2CH{=}\underset{CH_3}{C}CH_2)_2$ | 306 | < 0.005(6) |
| 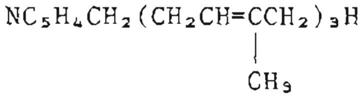 $NC_5H_4CH_2(CH_2CH{=}\underset{CH_3}{C}CH_2)_3H$ | 306 | < 0.005(6) |

---

[a] In 0.1 M trifluoroacetic acid, ambient temperature. Solutions contained, in addition, 0.015 M Cu(II); $[Cr(III)] = [Cu(I)]_0$.

[b] Number of individual runs given in parentheses; error limits are average deviations from mean values.

the absorbed light $I_a = 0.5 - 18.6 \times 10^{-6}$ ein sec$^{-1}$. All irradiations were performed at 306 nm in the Cu(I)-olefin ($\pi$*)-charge transfer band (Figure 20).

Photoredox quantum yields resulting from the irradiation of $A_5$Co(III)L ions at 306 nm were determined both by the method of Kitson[23] and the disappearance of the visible absorption band. Only in the cases of the large alkyl ligands were these quantum yields significant. Quantum yields for this process were calculated from equation 4 (page 35) and are 0.1 for both isoprenylamines. Quantum yields for other ligands were negligible.

All reactant solutions used in these studies contained (Cu(II)) = $1.5 \times 10^{-2}$ M, (Cr(III)) = $0.2 - 2.0 \times 10^{-3}$ M; reaction media were 0.1 M $HClO_4$ for the alkylamine complexes and 0.1 M HTFA for the alkylpyridine complexes. Reaction conditions and yields are given in Tables 15 and 16. Solutions used in the LMCT quantum yields (blanks) contained Cu(II) ions in place of the corresponding amount of Cu(I) ion which would be present in an experimental run of the $A_5$Co(III)(-Cu(I)) binuclear ion. The additional Cu(II) ion in this case was initially present as Cu(I) (generated by the usual method)[24] and the sample oxygenated to destroy the Cu(I) ion and repurged of $O_2$ with argon before irradiation.

$A_5$Co(III)alkylammine and $A_5$Co(III)alkylpyridine complexes were not reduced by Cu(I) in the absence of light, consistent with previous findings on Co(III)-Cu(I) binuclear ions of $A_5$Co(III) alkenoic acids and Cu(I).[16]

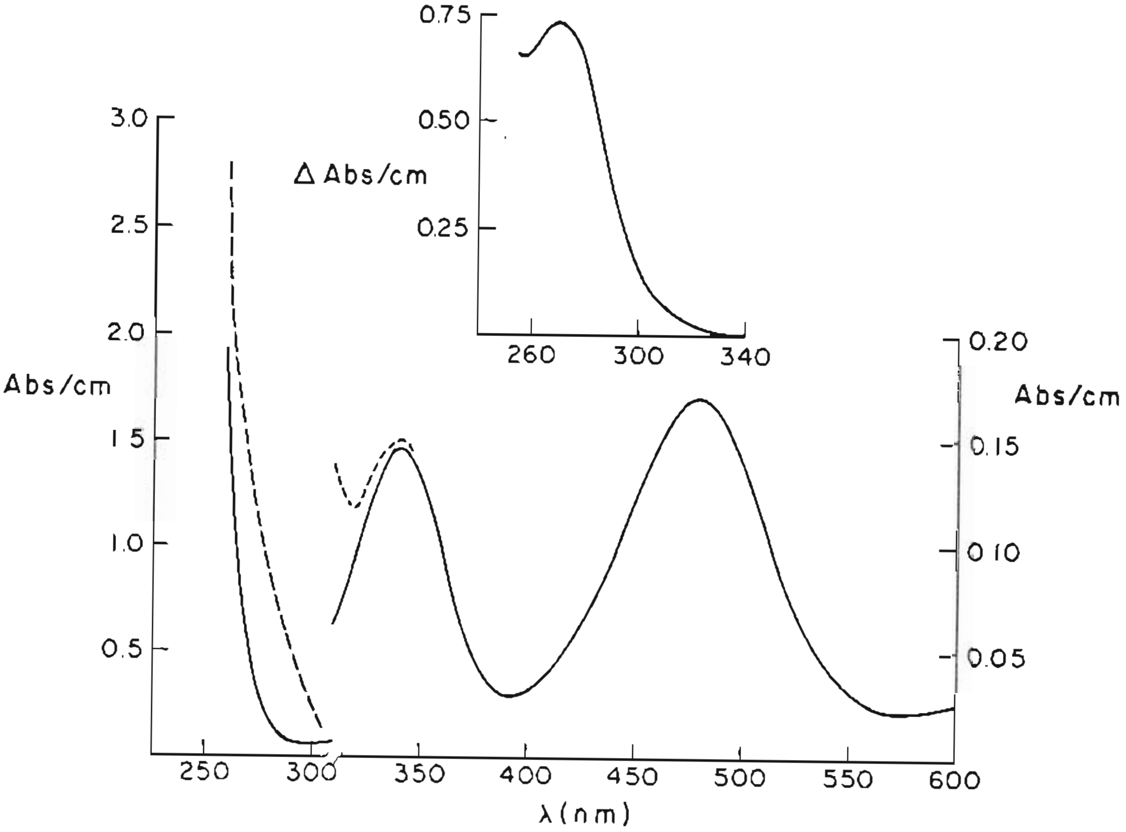

Figure 20. Electronic absorption spectra of $A_5Co(III)$-1-amino-5-hexene and Cu(I) ions solid line, $A_5Co(III)H_2N(CH_2)_4CH=CH_2$; dashed line $A_5Co(III)H_2N(CH_2)_4CH=CH_2$ and Cu(I) ions in 0.1 M $HClO_4$.

TABLE 15

Summary of Conditions and Quantum Yield for Photolysis of $A_5Co(III)L-Cu(I)$ Alkylpyridine Binuclear Ions[a]

| Ligand (L) | $10^3 \cdot [Cu(I)]$(M) | $10^3 \cdot [Co(III)]$(M) | $\phi$[b] |
|---|---|---|---|
| $NC_5H_4(CH_2)_2CH=CH_2$ | 0.9 | 0.9 | 0.16 |
| | 2.0 | 3.68 | 0.10 |
| | | 5.0 | 0.20 |
| | | 8.5 | 0.12 |
| $NC_5H_4(CH_2)_3CH=CH_2$ | 0.9 | 0.9 | 0.14 |
| | 2.0 | 3.5 | 0.08 |
| | | 8.5 | 0.09 |
| $NC_5H_4(CH_2)_4CH=CH_2$[c] | 0.9 | 0.9 | 0.08 |
| | 2.0 | 3.5 | 0.04 |
| | | 8.5 | 0.03 |

[a] In 0.1 M trifluoroacetic acid, ambient temperature.

[b] In addition 0.015 M Cu(II) and $[Cr(III)] = [Cu(I)]_0$ are present.

[c] Values listed in Table 14 for other alkylpyridine derivatives were run under the same conditions as yields in this table were less than the confidence of the experimental technique.

## TABLE 16

Summary of Conditions and Quantum Yields for Photolysis of $A_5Co(III)L-Cu(I)$ Aminoalkene Binuclear Ions[a]

| Ligand | $10^4 \cdot [Cu(I)]$ (M) | $10^4 \cdot [Co(III)]$ (M) | $\Phi$[b] |
|---|---|---|---|
| $H_2N(CH_2)_3CH=CH_2$ | 3.0 | 5.6 | 0.28 |
| | | | 0.31 |
| | 3.0 | 8.0 | 0.31 |
| | | | 0.39 |
| | | | 0.39 |
| | 4.0 | 25.0 | 0.32 |
| | | | 0.35 |
| $H_2N(CH_2)_4CH=CH_2$ | 3.2 | 5.0 | 0.30 |
| | | | 0.30 |
| | | 11.2 | 0.30 |
| | | | 0.24 |
| | 7.6 | 12.0 | 0.17 |
| | | | 0.20 |
| | | 27.6 | 0.24 |
| | | | 0.18 |
| $H_2N(CH_2)_6CH=CH_2$ | 3.0 | 5.6 | 0.03 |
| | | | 0.04 |
| | 6.0 | 27.0 | 0.04 |
| | | | 0.05 |
| | 10.0 | 30.0 | 0.03 |
| | | | 0.02 |
| | | | 0.04 |
| | | | 0.05 |
| $H_2N(CH_2)_8CH=CH_2$ | 5.0 | 9.0 | 0.03 |
| | | | 0.0 |
| | 8.0 | 10.0 | 0.01 |
| | | | 0.0 |
| | 8.0 | 15.0 | 0.0 |
| | | | 0.0 |

TABLE 16, Continued:

| Ligand (L) | $10^4\cdot$[Cu(I)](M) | $10^4\cdot$[Co(III)](M) | $\phi^b$ |
|---|---|---|---|
| $H_2N(CH_2CH{=}C{-}CH_2)_2H$ | 4.0 | 2.0 | 0.98 |
| | | | 0.75 |
| | | | 0.53 |
| | 3.0 | 3.4 | 0.80 |
| | | | 0.76 |
| | | | 0.73 |
| | 7.5 | 7.0 | 1.00 |
| | | | 0.89 |
| | | | 0.83 |
| | | | 0.70 |
| 25% ethanol | 3.0 | 3.0 | 0.69 |
| | | | 0.58 |
| | 5.0 | 6.8 | 0.71 |
| | 9.0 | 10.0 | 0.67 |
| | | | 0.72 |
| 83% ethanol | 3.0 | 3.75 | 0.51 |
| | | | 0.52 |
| | 9.0 | 10.1 | 0.48 |
| 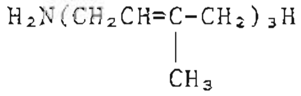 $H_2N(CH_2CH{=}\underset{\displaystyle CH_3}{\underset{\vert}{C}}{-}CH_2)_3H$ | 5.0 | 2.2 | 0.78 |
| | | | 1.00 |
| | | 5.1 | 0.80 |
| | | | 1.00 |
| | 8.0 | 8.0 | 1.0 |
| 50% ethanol | 7.0 | 8.3 | 0.42 |
| | | | 0.51 |
| | | | 0.52 |
| | | | 0.62 |
| 90% ethanol | 7.0 | 8.1 | 0.26 |
| | | | 0.36 |
| | | | 0.37 |

---

[a] All solutions contain 0.1 M $HClO_4$ and 0.015 M Cu(II) and [Cr(III)] = $[Cu(I)]_o$.

## Stoichiometry of Photoredox Process

Solutions containing binuclear ions at millimolar concentration were irradiated to 25% conversion to redox products, and the labilized ligands isolated and determined quantitatively. Results are listed in Table 17. Ligand yields correspond to the amount of Co(II) produced indicating no net reaction of the ligand as a consequence of electron transfer. The values listed are corrected for procedural losses, which were determined using standards, prepared to correspond to irradiated sample compositions at the end of 25% conversion to products, that were subjected to the same isolation procedures as the irradiated sample. Gas chromatographic analysis was used to determine ligand products; yields were corrected for ligands that arose from hydrolysis of $A_5Co(III)L$ complexes over the course of the measurements. The $A_5Co(III)$geranylamine number was also corrected for the amount of ligand labilized by photoexcitation of the $A_5Co(III)L$ complex at 306 nm. All recovered ligands co-chromatographed with samples of the organic compounds used in the $A_5Co(III)L$ complex ion syntheses.

## TABLE 17

Ligand Recovery from $A_5Co(III)L-Cu(I)$ Near U.V. Irradiations[a]

| Ligand (L) | $[A_5Co(III)L]$ Reacted mmol | Ligand recovered[b] mmol | (L)/(Co(III)) |
|---|---|---|---|
| $NC_5H_4(CH_2)_2CH{=}CH_2$ | 0.18 | 0.17 | 0.94 |
| $NH_2(CH_2)_3CH{=}CH_2$ | 0.16 | 0.15 | 0.94 |
| $NH_2(CH_2)_4CH{=}CH_2$ | 0.21 | 0.19 | 0.90 |
| 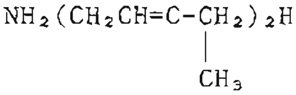 $NH_2(CH_2CH{=}\underset{\underset{CH_3}{\vert}}{C}{-}CH_2)_2H$ | 0.24, 0.19 | 0.21, 0.17[c] | 0.88, 0.90 |

---

[a] Experimental information given in text.

[b] Corrected for losses incurred in experimental procedure, and reactions other than those from Cu → L band irradiations.

[c] It is assumed in this reaction that the high quantum yield (0.1) for $Co^{2+}$ by reactions other than those from Cu(I) → L irradiation results in ligand destruction.

# CHAPTER 5

# DISCUSSION

## Cuprous Ion Reduction of Pyridinepentaammineruthenium(III) Ions

In the reaction between $A_5Ru(III)vp$ and Cu(I) ions, the ion association step (K, Scheme III) is due to Cu(I)-$\pi$-complexation of the olefin group. This is justified by the following: (a) comparison of thermodynamic parameters found for ion association with other olefin containing ions gave similar values; (b) no evidence of ion association was found for association of Cu(I) with Ru(III) ions lacking olefin-containing ligands.[13]

In this case binuclear ion formation can be treated as an equilibrium step preceding electron transfer; Cu(I)-olefin ligand association is rapid, approaching diffusion controlled limits.[34] As outlined in Scheme III, electron transfer between Cu(I) and $A_5Ru(III)vp$ can occur via an intramolecular ($k_a$) or intermolecular ($k_b$) pathway. In this case, the reaction pathway must be almost entirely intramolecular as the following arguments will show. Reduction of $A_5Ru(III)etpy$ ion by Cu(I) ion gives an estimate of the intermolecular pathway because no $\pi$-complexation by Cu(I) is possible. A number of $A_5Ru(III)$-4-alkylpyridine substituent containing ions of $A_5Ru(III)$ have been studied in reaction with Cu(I) ion resulting in essentially the same rate constant for each pair of reactant ions.[35] Thus no unusual steric constraint to electron transfer is expected from the presence of the ethyl group. In another reaction pair, $A_5Ru(III)py$ reacting with Cu(I)-π-allyl alcohol, there appears no enhanced activity for Cu(I) based simply on olefin-π-coordination (Table 10). In fact, the rate of electron transfer is reduced, presumably due to stabilization of Cu(I) by olefin complexation.*

From this data the intermolecular rate constant for the $A_5Ru(II)vp$ -Cu(I) reaction $k_b \approx 5.4\ M^{-1}s^{-1}$ at 23°C using the experimentally determined values, $k' = 0.24\ s^{-1}$ and $k = 1300\ M^{-1}$ and the contribution from pathway $k_b$ is calculated to be from Scheme III only 2% of the total reaction.

The arguments presented allow for a pathway for which π-complexation by Cu(I) ion is required for electron transfer. This does not mean, however, that this coordination is maintained in the activated complex in which electron transfer occurs. The lifetime of Cu(I)-olefin complexes is on the order of microseconds[34] so that dissociation or substitution and reassociation at another site in approaching the activated complex could be possible (See equation 5 on page 76).

---

*Under the conditions of the experiment ($5 \times 10^{-3}$ M allyl alcohol) Cu(I) is completely π-complexed ($K = 5 \times 10^{4}\ M^{-1}$ at 23°C, $\mu = 0.1$ M).[36] The activation free energy for reduction of $A_5Ru(III)py$ ion by Cu(I) π-allyl alcohol is greater than that of Cu(I) reduction of $A_5Ru(III)$ etpy by 1.4 kcalßmol at 23°C. This can be understood by considering that π-complexation stabilizes the Cu(I) oxidation state by 6.4 kcal/mol, thus reducing the driving force for the reaction.

$$\begin{aligned} &\mathrm{A_5Ru(III)vp + Cu(I)} \overset{k_a}{\rightleftharpoons} \mathrm{A_5Ru(III)vp(\pi)Cu(I)} \\ &\overset{\text{fast}}{\rightleftharpoons} \mathrm{A_5Ru(III)vp{\bullet}Cu(I)} \rightleftharpoons \mathrm{A_5Ru(II)vp + Cu(II)} \end{aligned} \tag{5}$$

Such a reaction coordinate is unlikely; it assumes that geometries allowing for electron transfer would be obtained that are unattainable by simple direct pairing. Without the essential binding sequence the system would gain no energetic advantage by such a pathway, the net result being pathway $k_b$, which has been shown to be too slow to account for the observed rate. Ultimately then, the conclusion must be that the Cu(I)-olefin π bond is maintained in the activated complex for electron transfer.[13]

## Thermodynamic Electron Transfer Parameters

Activation parameters for intramolecular electron transfer in binuclear ions are listed in Table 18. Other than the $A_5Ru(III)vp$-$Cu(I)$ entry, all $\Delta S^\ddagger$ values are near zero. Entropy changes involving bond compression and stretching in the activated complex will more than likely compensate, or be small in magnitude. Based on calculations for binuclear ion formation, formation entropies are sensitive to electronic effects. These effects as calculated turn out to be small for the binuclear ion studied here.[13] In the likelihood of small or no specific solvation e-fects involved in binuclear ion formation, the contribution from specific solvent restructuring in forming the transition state should be negligible, large solvent

## TABLE 18

### Activation Parameters for Intramolecular Electron Transfer

| Ion | $\Delta H^{\ddagger}_{et}$ (kcal/mol) | $\Delta S^{\ddagger}_{et}$ [c] (e.u.) | Reference |
|---|---|---|---|
| $A_5Ru(III)$-4-vinylpyridine•CuI | 15.1 ± 0.25 | -10 ± 4[d] | This work |
| Ro-4,4'-bipyridine-$A_4Ru(II)OH_2$, etc.[a] | 20 | +3 to -1 | 12b |
| Ro-NTA-Fe(II)[b] | 18.7 ± 1.3 | 0 ± 4 | 11 |
| $(en)_2Co(III)(SCH_2CO_2)Cu(I)$(S-bridged) | 21.4 ± 0.4 | 1.0 ± 2.5 | 46 |
| $A_5Co(III)py$•$(CN)_6Fe(II)$ | 21.7 ± 2.2 | 5.8 ± 7 | 47 |

[a] For π-conjugated bridging ligands.

[b] NTA = nitrilotriacetate.

[c] At 25°C, except where noted.

[d] 23°C.

effects having been accounted for in binuclear ion formation. Contributions to $\Delta S^{\ddagger}$ should therefore be small for the relatively little charge redistribution attending approach to the transition state. This is reasonable in light of some calculations by Marcus for the ferric and ferrous ion electron exchange reactions.[37] Here the solvent-ion atmosphere reorganization contributes only about 0.5 e.u. to $\Delta S^{\ddagger}$. Effects on low probability for electron transfer arising from electronic considerations (nonadiabaticity) during the lifetime of the activated complex can give rise to negative $\Delta S^{\ddagger}$ values.[13,37] For reactions where inner- and outer-coordination sphere reorganization give small contributions to the entropy terms, the magnitude of $\Delta S^{\ddagger}_{et}$ can be taken as a direct measure of the degree of nonadiabaticity in electron transfer, i.e., with $\Delta S^{\ddagger}_{et} \approx 0$ electron transfer is adiabatic.[38]

The $A_5Ru(III)vp$-$Cu(I)$ binuclear system explored in this study has a redox activation entropy much less than zero, suggesting nonadiabatic electron transfer. Of course this may be due to a very large contribution by restructuring of the solvent during the Cu(I) to Cu(II) coordination geometry change in the activation process. Solvent perturbation studies may provide information to distinguish between these two effects. If solvent reorganization is a significant contribution it should be reflected in $\Delta S^{\ddagger}$ and in $\Delta H^{\ddagger}$. If there is a nonadiabatic electron transfer, then $\Delta S^{\ddagger}$ will reflect the solvent structure change, but this change will not be compensated for in $\Delta H^{\ddagger}$.[39]

For the binuclear ion system the overall activation parameters are: $\Delta H^{\ddagger} = \Delta H^{\circ}_{K} + \Delta H_{k'}{}^{\ddagger} = 5.4 \pm 1.9$ cal/mol; $\Delta S^{\ddagger} = \Delta S^{\circ}_{K} + \Delta S_{k'}{}^{\ddagger} = -28 \pm 10$ e.u. and are summarized in Table 11. These values are typical for redox reaction between like-charged ions similar to those found in Table 2. For other $A_5$Ru(III) = Cu(I) reactant pairs studied, it is seen that these values also fall within the range of values found for reaction between like-charged ions. The overall value for $\Delta H^{\ddagger}$ is seen to be small: the result of compensating $\Delta H^{\circ}_{K}$ and $\Delta H_{k'}{}^{\ddagger}$, as suggested would be the case by Taube.[5]

## Difference Absorption Measurements in the $A_5$Ru(III)vp-Cu(I) Binuclear Ion

In binuclear ions where electronic coupling between the metal centers is weak the electron can be considered vibrationally trapped at one site.[15] Absorption bands have been observed for such ions which have been ascribed to intervalence electron transfer (IT).[40] Hush and Hopfield have developed theoretical treatments for optical electron transfer.[14,15] Because of its relative simplicity, the theory of Hush is amenable to experimental verification using measured thermal and optical properties of weakly coupled binuclear ions. Use of the theory requires knowledge of activation parameters for the intrinsic electron transfer step. This has been achieved in the $A_5$Ru(III)vp-Cu(I) system.

Based on a simple oscillator model, Hush derived equation 6 for weakly coupled redox sites.[15,41]

$$E_{th} = (E_{op})^2 \beta 4(E_{op} - E_o) \qquad (6)$$

where $E_{op}$ is the energy maxima of an intervalence (metal to metal) charge transfer band (IT), $E_{th}$ is the activation energy for the thermal process and $E_o$ is the internal energy change of the system. Using the values obtained from kinetic and thermodynamic measurements, $E_{th}$ = 15.1 kcal/mole and $E_o$ values 2.53 cal/mole or -0.178 cal/mole[42] from the kinetic and thermodynamic measurements respectively, one obtains from equation 6 values of 500 nm and 471 nm for wavelength maxima corresponding to $E_{op}$, respectively. The broad nature of the band and calculated band maximum[33] (Figure 18) are consistent with its assignment at Cu(I) → Ru(III) intervalence transfer. This result may be fortuitous. Solvent perturbation studies are necessary to determine whether or not this actually is an IT. If it is, however, temperature dependence studies on its behavior would provide important information to test theories advanced for such IT bands.

## Photoinitiated Electron Transfer

Long range photoinitiated electron transfer is common in biological systems. An important consideration in attempting to understand this process is the maximum distance over which charge transfer can occur. The thermal and photochemical properties of $A_5Co(III)$-olefin-Cu(I) ions are convenient for probing electron transfer distances.

Although energetically favorable, the rate for Cu(I) reduction of Co(III) in these binuclear ions is extremely slow, for reasons discussed in reference 33. Photoinitiated reduction occurs, however, the extent of which in preliminary studies appeared to be a sensitive function of distance between redox centers.

Hurst and coworkers have shown that irradiation of the LMCT absorption band of the Cu(I)-olefin $\pi$ band in Co(III)-Cu(I) binuclear ions is the primary photoexcitation process(es) leading to chemical reaction in these systems.[16] In these aminoalkene systems investigated here, irradiation in the absence of Cu(I) (essentially into the ligand near uv excited state band, or into the ligand band itself) does not give Co(II) formation. The conclusion drawn is that Cu(I)-olefin charge transfer excitation is the only process leading to net electron transfer. In addition, the lack of variance of quantum yields over approximately 10-fold concentration ranges indicates that electron transfer is an intramolecular process.

A possible mechanism for electron transfer in these hydrocarbon bridged binuclear ions is "through space" charge transfer, i.e., across the excluded volume of the hydrocarbon chain. Formation of discrete ligand radical ion-intermediates is unlikely because ligands were recovered in near quantitative yields, i.e., equivalent to the amount of Co(II) produced. Thus, no evidence for formation of relatively long-lived radical intermediates capable of polymerization or destructive reactions was found. If electron transfer is long range, it is likely to occur by a "resonance-exchange" type of tunneling.

It must be remembered that irradiation at 306 nm corresponds to putting 93 kcal/mole of energy into the system, which is an exceptionally large driving force for reaction.

Another possibility for the observed reactions has been suggested by Hurst and coworkers.[9] The ligand chain may fold so that the olefin $\pi$-orbital overlaps directly the cobalt $\pi^*$ orbitals, giving rise to the short-range transfer of the type usually described for redox centers between pairs of coordination compounds. The observation of decreasing quantum yield with increasing chain length can support either mechanism. In the former case the increasing median distance of the Cu(I) olefin from the Co(III) center can be associated with decreasing probability for transfer. In the latter case the distribution of molecules with metal centers in close proximity decreases with increasing chain length.

In other experiments on the effect of chain length on hydrogen abstraction by benzophenone it was found that quantum yields increased with increasing chain length.[43] The result was interpreted as indicating that the alkane chain came in contact with the reactive volue of the carbenyl group only for longer chains and it was suggested that shorter chains are more rigid than longer chains. In these experiments, chains shorter than 10 carbons gave no measureable quantum yields. Applying this observation to the Co(III)-Cu(I) ions it would seem that the population of conformational states allowing direct overlap of donor and acceptor orbitals is too small to account for measured redox quantum yields.

The results of quantum yields for photoinitiated electron transfer are plotted in Figure 21 against the number of carbons in the chain. The "carbon" number for the pyridine containing ligands was estimated assuming that the pyridine 4-carbon was equivalent to the α-carbon of the amine chain, i.e., that π-conjugated bonds in the pyridine ring did not contribute to its effective length. Calculations were made assuming a fully elongated chain with all bonds in the *trans* configuration. Given this conformational state, actual distance between metal centers can be estimated from carbon-carbon bond distance and angles and appropriate metal ligand distances.[10,46] A typical value, which is confessed to be somewhat arbitrary, for the pentenylamine bridging ligand is 6.4 Å.

Experiments using $A_5Co(III)$[2.2.2.]bicyclo-2-octene-5-methyl-5-carboxylate (K. A. Norton and J. K. Hurst, unpublished data) give large quantum yields for photoinitiated redox ($\phi$ = 0.9 and 0.7 for the *endo* and *exo* carboxylate isomers respectively, shown in Figure 22). Comparison of these yields with the lesser value obtained for $A_5Co(III)$ 5-amino-1-pentene (Table 12) which also has a 3-carbon alkane bridge, suggest either that the rigid geometry of the bicyclo system gives rise to a preferred configuration for photoredox, or that the hydrophobic nature of the *exo* bicyclo ring minimizes solvent quenching of the photoreactive state. Also it may not be appropriate to compare the yields obtained for carboxylate ligands with those of amines. It can be seen from models of the *endo* carboxylate isomer that the oxygen atoms come very close to the olefin and may mediate electron transfer;

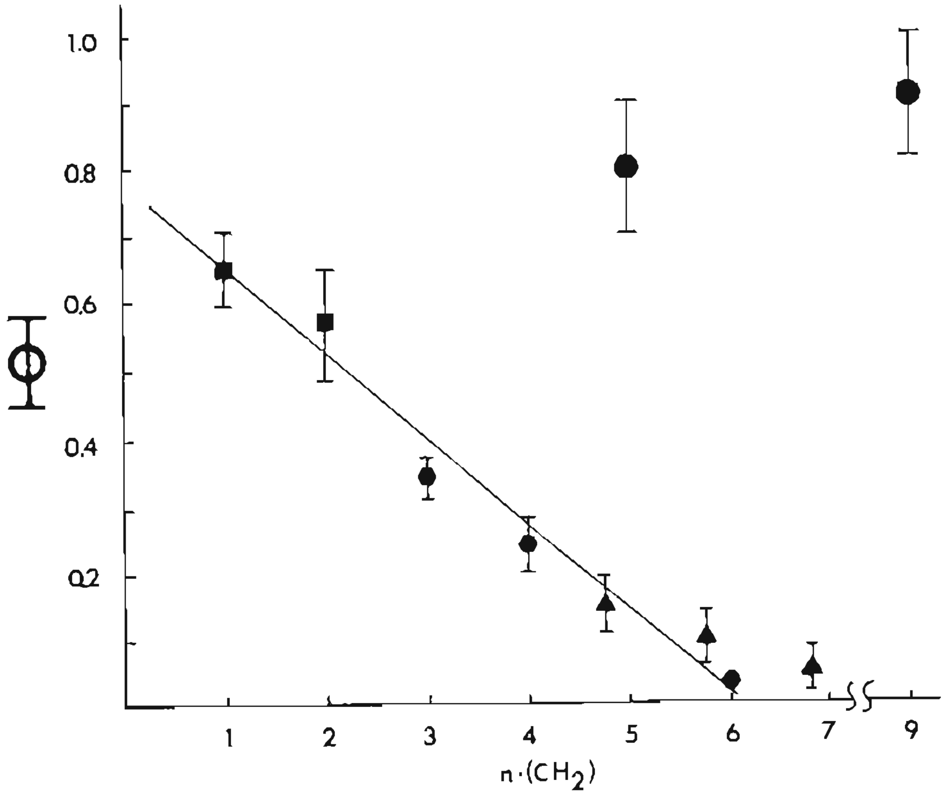

Figure 21. Plot of quantum yield vs. carbon number for Co(III)-Cu(I) binuclear ions; ● indicate amino-alkene bridged ions from this study; ■ are amino-alkene bridged ions from ref. 16; ● represent polyisoprenylamines; ▲ represent alkylpyridine bridged ions; quantum yield data taken from Tables 12 and 13.

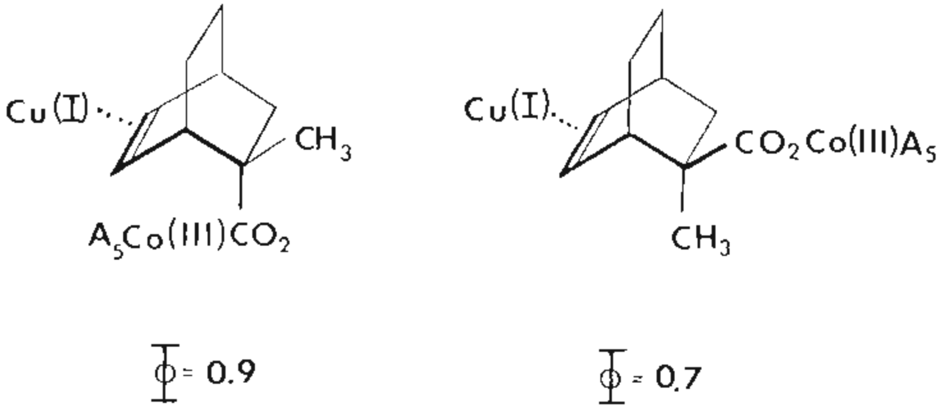

Figure 22. Photoinitiated redox quantum yields for the *exo* and *endo* isomers of $A_5Co(III)$[2.2.2.]bicyclo-2-octene-5-methyl-5-carboxylate.

in any event in this system the Cu(I) and Co(III) centers are in close proximity.

From most elementary considerations, aminoalkene and alkylpyridine bridging ligands of $A_5Co(III)$-Cu(I) binuclear ions can be viewed as flexible chains between centers of unequal mass. Because accurate conceptual models which take into specific account electrostatic, unequal end chain masses and perturbation of the local dielectric by highly charged ions do not exist, it is not yet possible to calculate the relative mean distribution of any configuration in the Co(III)-Cu(I) binuclear ions. Therefore the mean metal to metal distance over which electron transfer occurs in polymethylene based bridging ligands can be only estimated.

The relatively high quantum yields of Co(III)-Cu(I) binuclear ions containing polyisoprene bridging ligands suggests the operation of an alternate mechanism for electron transfer. The stoichiometries for Cu(I)-polyisoprenylpyridine binding have been determined to be 1:1 by Raman and the method of continuous variation studies, ruling out multiple site binding to account for the observed high quantum yields observed.[44] Construction of molecular models of polyisoprenylamines shows allowed close contact between olefins in folded conformations. This "stacking" of isoprene units has been suggested to participate in heme *a* of cyctochrome *c* oxidase,[17] and extended π-interaction facilitating long range electron transfer has basis in theory.[45]

In highly polar media it is expected that the hydrophobic nature of the polyisoprene ligand causes it to fold. Folding of the ligand could result in stacking of the olefins which presumably would leave only the terminal olefin available for binding.[44] The lack of concentration dependence of quantum yields, albeit over a limited range, suggests micellar formation is not an important factor.

The decrease in quantum yield, with increasing ethanol content of the solvent, could be the result of melting of specific conformations necessary for long range electron transfer. This decrease may be due, however, all or in part to greater quenching of the excited state by solvent. Therefore, comparison of quantum yields for polyisoprene bridged with polymethylene bridged Co(III)-Cu(I) binuclear ions, the results suggest a different mechanism for electron transfer obtains in the polyisoprene bridged ions--evidence suggesting extended $\pi$-interaction between metal sites in aqueous solution.

# CHAPTER 6

## SUMMARY

Photoinitiated electron transfer occurs in alkylpyridines and alkylamine bridged Co(III)-Cu(I) binuclear ions. An elementary model has been presented to note the effect of chain length on distance, as judged by quantum yield. Alkylpyridine bridging ligands behave as if the pyridine $\pi$-cloud facilitates electron transfer, i.e., it does not add to chain length. Additional evidence for $\pi$-orbital participation in electron transfer is suggested by high quantum yields for polyisoprene bridged binuclear ions; the high yields for the bicyclooctene carboxylate ligands, however, suggest that a different mechanism is in operation here as compared with the polymethylene bridged binuclear ions. Theoretical models of chain conformation are necessary now to specifically define the distance of electron transfer in these studies. Distances in the polymethylene bridged ions give significant quantum yields to suggest that electrons may transfer over distances approaching 10 Å, perhaps by the mechanism of electron tunneling.

Other work presented pertained to thermal and optical electron transfer. This information is necessary for understanding and testing theoretical models. Knowledge of entropy, enthalpy, distance and temperature dependence of optical transitions will eventually lead to an improved understanding of the fundamental nature of redox processes.

# REFERENCES

1. See, e.g., "Tunneling in Biological Systems," B. Chance, D. C. DeVault, H. Frauenfelder, R. A. Marcus, J. R. Schrieffer, N. Sutin, Eds.; Academic Press: New York, 1979 for current approaches and developments.
2. Taube, H.; Myers, H.; Rich, R. L. J. Am. Chem. Soc. 1953, 75, 4118.
3. Linck, R. G. "Survey of Progress in Chemistry," A. F. Scott, Ed.; Academic Press: New York, 1976; p. 89.
4. Langford, C. H.; Gray, H. B. "Ligand Substitution Reactions," W. A. Benjamin Inc.: New York, 1965.
5. Taube, H.; Gould, E. S. Acc. Chem. Res. 1969, 2, 321.
6. Movius, W. G.; Linck, R. G. J. Am. Chem. Soc. 1969, 91, 5394.
7. Seewald, D.; Sutin, N.; Watkins, K. O. J. Am. Chem. Soc. 1969, 91, 7307.
8. Cannon, R. D.; Early, T. J. Am. Chem. Soc. 1966, 88, 1872.
9. Diaz, H.; Taube, H. Inorg. Chem. 1970, 9, 1304.
10. Hurst, J. K.; Lane, R. H. J. Am. Chem. Soc. 1973, 95, 1703.
11. Cannon, R. D.; Gardiner, J. J. Am. Chem. Soc. 1970, 92, 3800.
12. a) Hurst, J. K. J. Am. Chem. Soc. 1976, 98, 4001. b) Fischer, H.; Tom, G. M.; Taube, H. J. Am. Chem. Soc. 1976, 98, 5512.
13. Norton, K. A.; Hurst, J. K. J. Am. Chem. Soc. 1978, 100, 7237.
14. Hopfield, J. J. Proc. Nat. Acad. Sci., USA 1974, 71, 3640.
15. Hush, N. S. Progr. Inorg. Chem. 1967, 8, 391.

16. Farr, J. K.; Hulett, L. G.; Lane, R. H.; Hurst, J. K. *J. Am. Chem. Soc*. 1975, *97*, 2654.

17. Caughy, W. S.; Smythe, G. A.; O'Keeffe, D. H.; Maskasky, J. E.; Smith, M. L. *J. Biol. Chem*. 1975, *250*, 7602.

18. Wiley, G. A.; Hershkowitz, R. L.; Rein, B. M.; Chung, B. C. *J. Am. Chem. Soc*. 1964, *86*, 964.

19. Brown, H. C.; Murphy, W. A. *J. Am. Chem. Soc*. 1951, *73*, 3308.

20. Roberts, J. D.; Mazur, R. H. *J. Am. Chem. Soc*. 1951, *73*, 2509.

21. Boehme, W. R.; Schipper, E.; Scharpf, W. G.; Nichols, J. *J. Am. Chem. Soc*. 1958, *80*, 5494.

22. Blicke, F. F.; Doorenbos, J. J. *J. Am. Chem. Soc*. 1954, *76*, 2317.

23. Kitson, R. E. *Anal. Chem*. 1950, *22*, 664.

24. Shaw, K.; Espenson, J. M. *Inorg. Chem*. 1968, *7*, 1614.

25. Faeder, E. J. Ph.D. Dissertation, Cornell University, New York, 1970, p. 70.

26. Massey, G. A.; Johnson, J. C. *J. Quant. Electron*. 1976, *QEY2*, 721.

27. Johnson, J. C.; Massey, G. A. *Appl. Opt*. 1978, *17*, 2268.

28. Calvert, J. G.; Pitts, J. N. Jr. "Photochemistry," Wiley: New York, 1966.

29. Stanbury, D. M.; Haas, O; Taube, H. *Inorg. Chem*. 1980, *19*, 518.

30. Lim, H. S.; Barclay, D. J.; Anson, F. C. *Inorg. Chem*. 1972, *11*, 1460.

31. Callahan, R. W.; Keene, F. R.; Meyer, T. J.; Salmon, D. J. *J. Am. Chem. Soc*. 1977, *99*, 1064.

32. Adams, R. N. "Electrochemistry at Solid Electrodes," Marcel Dekker: New York, 1969.

33. Taube, H. In "Tunneling in Biological Systems" (See Ref. 1).

34. Meyerstein, D. *Inorg. Chem.* 1975, *14*, 1716.

35. Norton, K. A.; Hulett, L. G.; Halko, D. J.; Hurst, J. K. In "Electron Tunneling in Biological Systems," University of Pennsylvania: Philadelphia, 1978.

36. Hartley, F. R. *Chem. Rev.* 1973, *73*, 163.

37. Waisman, E.; Worry, G.; Marcus, R. A. *J. Electroanal. Chem.* 1977, *82*, 9.

38. Reynolds, W. L.; Lumry, R. W. "Mechanisms of Electron Transfer," Ronald: New York, 1966.

39. Lumry, R.; Rajender, S. *Biopolymers* 1970, *9*, 1125.

40. Powers, M. J.; Meyer, T. J. *J. Am. Chem. Soc.* 1980, *102*, 1289.

41. Hush, N. S. *Electr. Chim. Acta* 1968, *13*, 1005.

42. Latimer, W. M. "Oxidation Potentials," 2nd ed. Prentice-Hall: Englewood Cliffs, NJ, 1952.

43. Winnik, M. A. *Acc. Chem. Res.* 1977, *10*, 173.

44. Halpern, J.; Orgel, L. E. *Disc. Far. Soc.* 1960, *29*, 32.

45. Hurst, J. K. *Biochemistry* 1979, *18*, 1504.

46. Farr, J. K.; Lane, R. H. *J. Chem. Soc. Chem. Comm.* 1977, 153.

47. Miralles, A. J.; Armstrong, R. E.; Haim, A. *J. Am. Chem. Soc.* 1977, *99*, 1416.

# BIOGRAPHICAL NOTE

Kenneth Alfred Norton, Jr. was born in Long Branch, New Jersey on August 8, 1952, first born of Kenneth A. and Claire B. Norton. He received a B.S. degree in Chemistry from Rider College, Lawrenceville, New Jersey in 1974. He then entered Southern Illinois University at Edwardsville where he received an M.S. degree in Chemistry for work involving enzyme hydrolysis of rigid phenyl ester substrates. He began study at the Oregon Graduate Center in the fall of 1976. In 1980 he began a Welch postdoctoral fellowship in the laboratory of William Woodruff at University of Texas at Austin. Presently his primary scientific interests are in areas of photoinitiated and thermal electron transfer in homogenous and heterogenous solutions, in enzymic conformational changes leading to reactive states, and in ultrafast kinetic studies of excited state reaction intermediates.